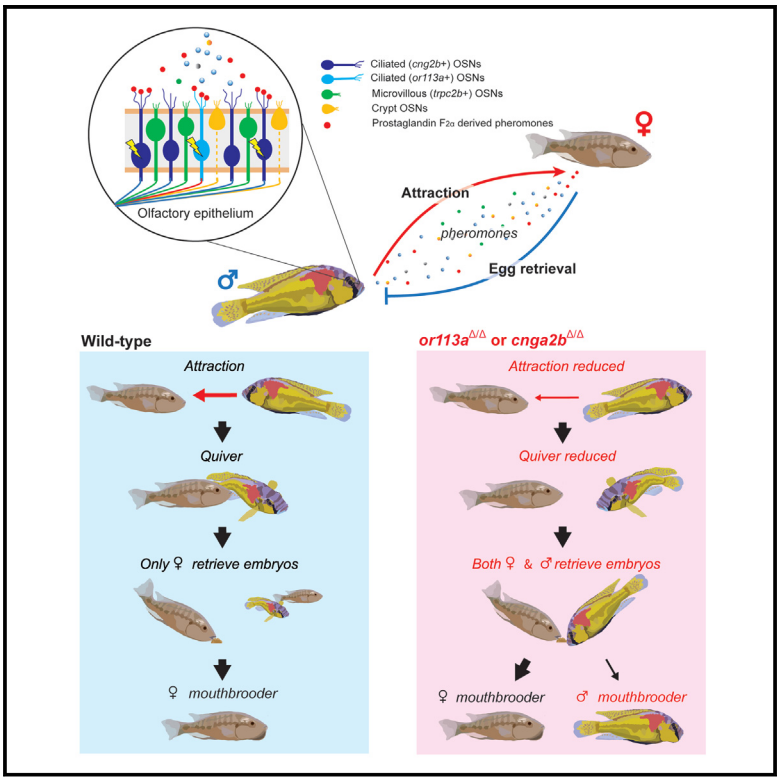
Article

Current Biology

A pheromone receptor in cichlid fish mediates attraction to females but inhibits male parental care

Graphical abstract



Highlights

- Single-nucleus RNA sequencing reveals cell types in the cichlid olfactory epithelium
- Male detection of fertile females uses the ciliated sensory neuron channel Cnga2b
- Olfactory receptor Or113a detects fertile females, promoting male mating
- Males mutant for *cnga2b* or *or113a* initiate mouthbrooding care behavior

Authors

Cheng-Yu Li, Jessica M. Bowers, Theresa A. Alexander, Kristen A. Behrens, Peter Jackson, Cyrus J. Amini, Scott A. Juntti

Correspondence

sjuntti@umd.edu

In brief

Li et al. discover that male cichlid fish use the olfactory receptor Or113a to detect fertile female cues. Surprisingly, Or113a also mediates males' avoidance of parental care. In CRISPR-generated mutant cichlids, males retrieve eggs and mouthbrood them, a behavior normally displayed only by females.

Li et al., 2024, Current Biology *34*, 3866–3880
September 9, 2024 © 2024 Elsevier Inc. All rights are reserved, including those for text and data mining, AI training, and similar technologies.
https://doi.org/10.1016/j.cub.2024.07.029

CellPress

CellPress

Current Biology

Article

A pheromone receptor in cichlid fish mediates attraction to females but inhibits male parental care

Cheng-Yu Li,[1] Jessica M. Bowers,[1] Theresa A. Alexander,[1] Kristen A. Behrens,[1] Peter Jackson,[1] Cyrus J. Amini,[1] and Scott A. Juntti[1,2,3,*]

[1]Department of Biology, University of Maryland, College Park, MD 20742, USA
[2]X (formerly Twitter): @ScottJuntti
[3]Lead contact
*Correspondence: sjuntti@umd.edu
https://doi.org/10.1016/j.cub.2024.07.029

SUMMARY

Reproductive behaviors differ across species, but the mechanisms that control variation in mating and parental care systems remain unclear. In many animal species, pheromones guide mating and parental care. However, it is not well understood how vertebrate pheromone signaling evolution can lead to new reproductive behavior strategies. In fishes, prostaglandin $F_{2\alpha}$ ($PGF_{2\alpha}$) drives mating and reproductive pheromone signaling in fertile females, but this pheromonal activity appears restricted to specific lineages, and it remains unknown how a female fertility pheromone is sensed for most fish species. Here, we utilize single-cell transcriptomics and CRISPR gene editing in a cichlid fish model to identify and test the roles of key genes involved in olfactory sensing of reproductive cues. We find that a pheromone receptor, Or113a, detects fertile cichlid females and thereby promotes male attraction and mating behavior, sensing a ligand other than $PGF_{2\alpha}$. Furthermore, while cichlid fishes exhibit extensive parental care, for most species, care is provided solely by females. We find that males initiate mouthbrooding parental care if they have disrupted signaling in ciliated sensory neurons due to *cnga2b* mutation or if *or113a* is inactivated. Together, these results show that distinct mechanisms of pheromonal signaling drive reproductive behaviors across taxa. Additionally, these findings indicate that a single pheromone receptor has gained a novel role in behavior regulation, driving avoidance of paternal care among haplochromine cichlid fishes. Lastly, a sexually dimorphic, evolutionarily derived parental behavior is controlled by central circuits present in both sexes, while olfactory signals gate this behavior in a sex-specific manner.

INTRODUCTION

Social behavior is guided by within-species signals and, for many species, pheromonal compounds play a major role.[1] Male and female animals typically display distinct behaviors during mate choice, courtship, gamete release, and parental care, with pheromone signaling guiding these behaviors in numerous species.[2–4] However, it remains unclear to what extent behavioral effects regulated by pheromone receptors are shared across species. It is also uncertain whether changes in peripheral sensory systems or central circuitry drive the evolution of behavioral strategies for reproduction.[5–10] Thus, a deep understanding of pheromone-guided social behavior requires an evolutionary perspective.[11] Reproductive behaviors, including mating and parenting, are useful phenotypes with which to seek mechanistic insight due to their robust nature, regulation by hormones and pheromones, and evolutionary lability. Fish and amphibians exhibit variation in parental care strategy, providing opportunities to identify causes of behavioral differences. Among these classes, ~10%–30% of species exhibit parental care, and within these, males, females, or both together may provide care.[12–14] Evolutionary transitions to male care are hypothesized to result from a female-biased operational sex ratio or challenging environments.[15] In search of proximate mechanisms, comparisons within species across males that provide varying levels of care reveal contributions of gonadal hormones and the neuropeptides vasopressin and galanin.[16–25] Among voles and the *Peromyscus* genus of mice, enhanced male parental care is found in pair-bonding species. Variation in male contribution to parenting is pronounced in this clade, and vasopressin has been implicated in its control through pharmacology and genomic mapping.[10,26] Genetic disruption of the mouse vomeronasal organ (VNO), an important pheromone sensor, results in altered sociosexual behaviors,[27,28] as does silencing of the main olfactory epithelium (OE).[29,30] Although virgin male mice (*Mus musculus*) typically act aggressively toward pups, following inactivation of the Trpc2 channel essential for normal VNO function, males reduce aggression and exhibit parental care.[31] The ability of mice to exhibit reproductive behaviors typical of the opposite sex following sensory manipulations implies that both sexes retain functional neural circuitry for social behaviors, including parenting.[7,31] It also raises the possibility

 © 2024 Elsevier Inc.
All rights are reserved, including those for text and data mining, AI training, and similar technologies.

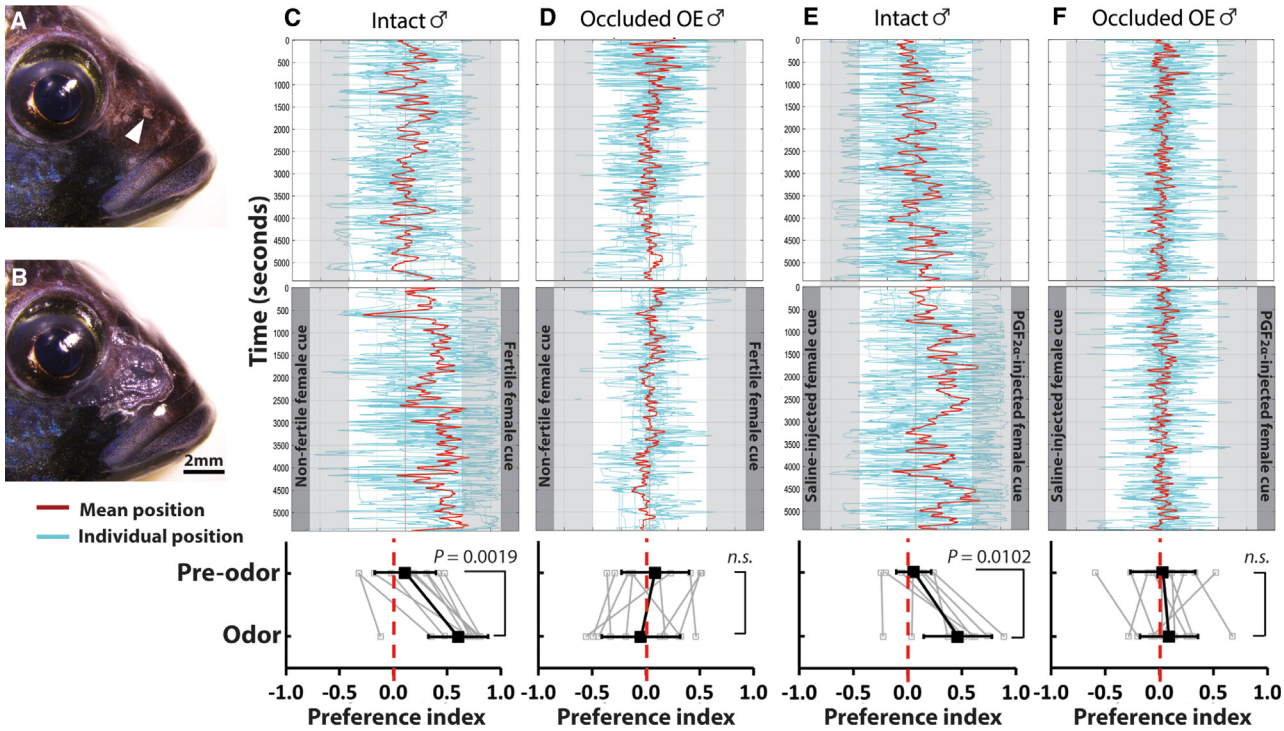


Figure 1. Olfactory epithelium is necessary for attraction to the $PGF_{2\alpha}$-initiated fertility signal

(A) Olfactory nare (arrowhead) is the sole entry point for water to the cichlid olfactory epithelium.

(B) Occluded olfactory epithelium using Vetbond tissue adhesive.

(C–F) Preference for water conditioned by fertile or $PGF_{2\alpha}$-injected females vs. non-fertile females. Upper panels show fish behavior prior to odor exposure, lower panels are time following odor delivery. Cyan lines represent individual trials; red line represents mean position.

(C and E) (C) Males prefer naturally fertile and (E) $PGF_{2\alpha}$-injected non-fertile female-conditioned water over non-fertile female cues.

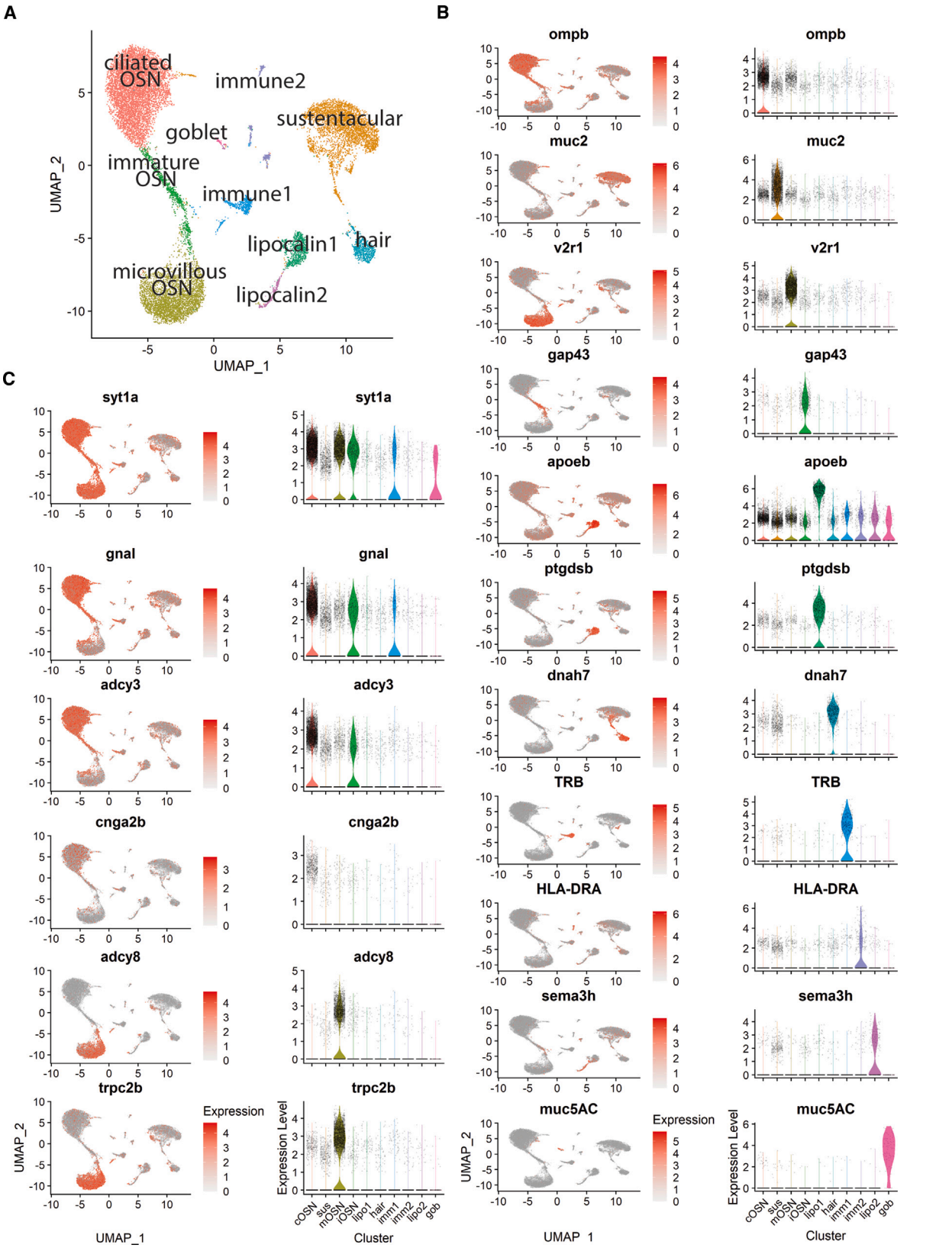
(D and F) (D) Males with bilaterally occluded nares do not prefer naturally fertile or (F) $PGF_{2\alpha}$-injected non-fertile female-conditioned water compared with non-fertile-female water. Overall preferences are summarized at the bottom: gray squares and lines represent preference index in individual trials, while black squares and lines represent mean ± SD. Mann-Whitney U test, n = 10 fish per experiment. n.s., not significant.

See also Figure S9 and Table S1.

that reproductive behavior patterns may evolve in response to changes in sensory perception.

Cichlid fish offer an attractive system to identify mechanisms that regulate social signaling because they exhibit extensive, quantifiable social behaviors in the lab. Furthermore, the ~2,000 species in the cichlid family results from the most explosive species radiation among vertebrates, and these species vary in numerous social behaviors, including mate preference and parental care strategies.[32,33] Finally, genome sequences for hundreds of these species are publicly available, and they can be readily manipulated through transgenesis and CRISPR-Cas genome editing.[34–37] Prior studies in the genetically manipulable cichlid *Astatotilapia burtoni* revealed neural populations in the brain that are activated during female parental care.[38] To understand how processing of social signals varies across species with divergent levels of parental care, it is essential to identify the sensory signals that regulate the activity of central parenting circuits.

Reproductive behaviors in vertebrates change as hormone titers fluctuate across the ovarian cycle. These hormones impact female behaviors directly and also regulate the cyclical release of pheromones into the environment, affecting male reproductive behaviors.[39–41] Among teleost fishes, ovulation initiates the production of prostaglandin $F_{2\alpha}$ ($PGF_{2\alpha}$) by the female reproductive tract.[42] $PGF_{2\alpha}$ initiates female mating behavior, and olfactory cues from these fertile females elicit behavioral changes among bystanders.[37,43–45] Males are attracted to fertile females' cues, and these odor cues enhance courtship and territorial behavior.[46,47] Zebrafish and other otophysan fishes detect $PGF_{2\alpha}$ using the olfactory receptor (OR) Or114-1 (aka Or55d1) and its paralog Or114-2.[47] However, while $PGF_{2\alpha}$ likely functions as a hormone across fish, most species are probably insensitive to environmental $PGF_{2\alpha}$.[39,48,49] We previously showed that the loss of $PGF_{2\alpha}$ sensitivity is associated with the loss of *or114* gene paralogs ~150 million years ago (mya), in the neoteleost lineage, which includes cichlids, gobies, and cod.[50,51] However, $PGF_{2\alpha}$ initiates the release of a distinct molecule or molecules that attract male *A. burtoni*.[50] Thus, coevolution of pheromones and their ORs has occurred across fishes, a process that could enable taxon-specific identification of potential mates. As a result, we seek to identify an alternative pheromone receptor to provide insight into the evolution of pheromone signaling. Furthermore, the identification of a receptor that detects fertile females would enable a direct test of whether this receptor mediates only attraction or has pleiotropic effects on other reproductive behaviors, including parenting.



(legend on next page)

CellPress

Here, we identify the ciliated olfactory sensory neurons (OSNs) as detectors of female fertility pheromones that control male attraction. Surprisingly, these neurons also control the inhibition of parental behavior in males. Moreover, we identify a specific OR, Or113a (Or55a1), that is necessary for detection of the $PGF_{2\alpha}$-derived pheromone in the cichlid *A. burtoni*. Deletion of this receptor leads to mating deficits in males and also results in male retrieval of eggs during spawning, a parental behavior that is performed exclusively by females in all haplochromine cichlids (i.e., the ~1,000 species most closely related to *A. burtoni* that have speciated most rapidly). Together, our results suggest a model in which a $PGF_{2\alpha}$-derived female fertility cue activates Or113a, and this signaling both attracts males and inhibits male parental care.

RESULTS

A cell atlas of cichlid OE

Our previous work indicated that the loss of *or114* is responsible for the olfactory insensitivity of many fish species to free $PGF_{2\alpha}$ but that $PGF_{2\alpha}$ initiates pheromonal signaling via an alternate pathway.[50] To identify a sensory mechanism in cichlids, we first asked whether this attraction to fertile females requires the OE. Male cichlids with occluded nares (Figures 1A and 1B) failed to exhibit an olfactory preference for water conditioned by fertile females or non-fertile females injected with $PGF_{2\alpha}$ (Figures 1C–1F). To gain insight into the cellular mechanism, we sought to determine which class of OSN detects the attractive fertility pheromone. Among fish, most OSNs fall into three classes: ciliated OSNs that express OR or trace-amine-associated receptors (TAARs), microvillous cells that express V2R-type vomeronasal receptors, and crypt cells that express a V1R receptor.[52] We sought to characterize these cell types to identify essential signal transduction components that, when eliminated, would silence individual OSN classes. We used single-nucleus RNA sequencing (snRNA-seq; n = 8 fish) to profile the expression pattern of ~17,000 cells in the OE (Figures 2A and 2B). We used Gene Ontology (GO) analysis on the top differentially expressed genes in each cluster and found that distinct clusters corresponded to known neuronal and non-neuronal cell types (Table S1). We used *in situ* hybridization (ISH) to label transcripts enriched in individual clusters to gain insight into their cellular function (Figure 3). In addition to putative sustentacular cells (*muc2*$^+$), we found other non-neuronal cell types: apparent goblet secretory cells (*muc5ac*$^+$), cells enriched for production of lipocalins (*ptgdsb*$^+$, *apoeb*$^+$), non-neuronal hair cells (*dnah7*$^+$), and immune cells (*TRB*$^+$ cells, *HLA-DRA*$^+$ cells) (Figure 3A). When we analyzed neurons, as marked by *syt1a* expression, we identified three clear groups of cells, which we classified into immature neurons, ciliated OSNs, and microvillous OSNs (Figure 2C). Immature neurons are enriched for *gap43*, a marker previously shown in zebrafish to label these cells.[53] These cells are located at the distal edges of the OE (Figure 3A), suggesting that, following fate determination, they migrate tangentially to their final positions in the sensory cell layers in a manner similar to that shown in zebrafish.[53] Microvillous neurons express *v2r1* (a receptor expressed in all zebrafish microvillous cells[54]), *trpc2b*, and *adcy8* (Figure 2C). These markers are expressed in cells of the apical OE layer (Figure 3B), as previously shown for zebrafish.[55,56] Ciliated neurons express *cnga2b*, *ompb*, *adcy3*, *OR*, and TAAR genes. These cells are expressed in a more basal layer than microvillous neurons (Figure 3B), in keeping with previous findings.[55,56] When we reclustered putative neurons, we found that a subset of neurons are enriched for markers of crypt cells,[57,58] including *ora4*, *ntrk2a*, and *gnai1* (*gi1b*) (Figures S1A–S1C). However, this cell group of rare neurons comprising 1%–2% of neurons in fish[59–61] was not well resolved and so we did not pursue this class further.

Previous work has shown that Trpc2 and Cnga2 are critical channels in mice for the function of microvillous and ciliated neurons, respectively.[27–29] Due to the teleost whole-genome duplication, however, it is unclear which paralogs are responsible for the depolarization of these cells. Two *cnga2* paralogs are retained in cichlids (Figure S3B). We find that *cnga2b*, but not *cnga2a*, is expressed in ciliated neurons (Figures 3B, S1B, and S2B) and that *cnga2b* is not detected elsewhere in the brain (Figure S2A). Microvillous neurons express *trpc2b*, while its paralog *trpc2a* appears to have been generated during the teleost whole-genome duplication, then lost in neoteleosts following the split from the otophysan lineage (Figure S3A). *Trpc2b* is expressed in the OE (Figures 3B and S2D), but we did not detect it in the brain by ISH (Figure S2C). Thus, we reasoned that *trpc2b* or *cnga2b* deletion would lead to animals with silenced microvillous or ciliated neurons, respectively.

Functional genetic interrogation of fertility pheromone sensation

We asked which population of OSNs detect reproductive female odors by colabeling for the neural activation marker *fosab* (activity-induced teleost homolog of *cfos*[37]) and *trpc2b* transcripts in OE following olfactory stimulation. We found that most *fosab*$^+$ cells are located basal to the *trpc2b*$^+$ microvillous layer following stimulation by water conditioned by fertile, $PGF_{2\alpha}$-injected females, consistent with a model in which ciliated OSNs are important for sensing reproductive odors (Figure S4A). To directly test this hypothesis, we used CRISPR in *A. burtoni*[62] to introduce mutations in coding regions of cichlid *trpc2b* and *cnga2b* (Figures 4A and 4B). We targeted regions 5′ to the predicted channel pore regions previously shown to be essential for the function of the mouse gene orthologs.[27,63] We found that males

Figure 2. Single-nucleus RNA-seq reveals discrete cell types in the cichlid olfactory epithelium

(A) Uniform manifold approximation and projection (UMAP) visualization of cells in the cichlid olfactory epithelium (17,284 nuclei from 8 cichlids) identifying 10 distinct cell types.

(B) UMAP and violin plots representing expression of selected markers for each cluster, ciliated OSN; sus, sustentacular cell; mOSN, microvillous OSN; iOSN, immature OSN; lipo1, lipocalin cell type 1; imm1, immune cell type 1; imm2, immune cell type 2; lipo2, lipocalin cell type 2; gob, goblet cell. Expression is represented as the normalized, natural log-transformed number of transcripts in each cell.

(C) UMAP and violin plots representing expression of selected signal transduction genes in olfactory neuron populations.

See also Figures S1 and S9 and Table S1.

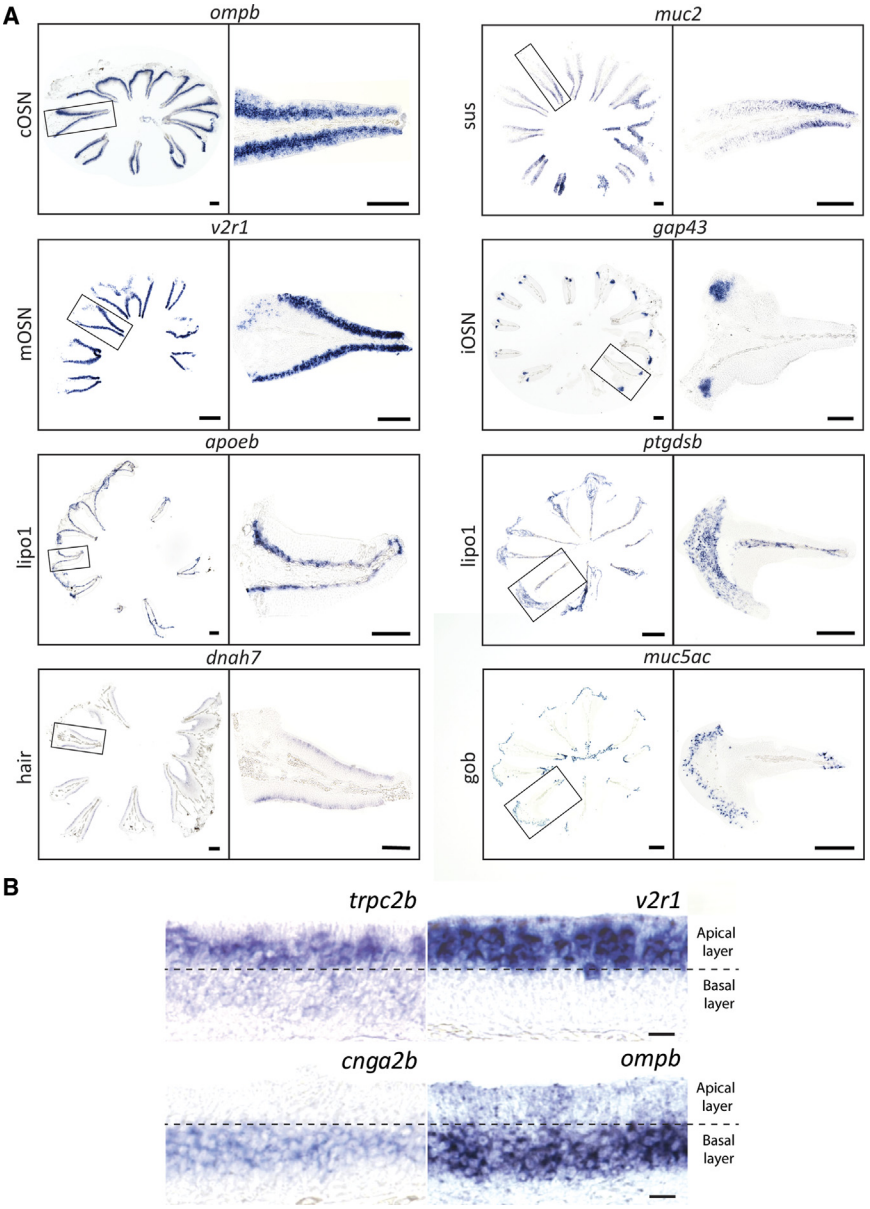


Figure 3. ISH detection of selected mRNA markers reveals the spatial arrangement of sensory and non-sensory cells in the olfactory epithelium

(A) Markers have distinct expression patterns and are specific to discrete cell types identified by single-nucleus RNA-seq. Scale bars, 100 μm.

(B) ISH for sensory transduction channels *trpc2b* and *cnga2b* in apical microvillous and basal ciliated olfactory neurons, respectively. Scale bars, 10 μm.

See also Figures S2 and S3.

carrying biallelic mutations for each of these genes have normal mass (Figures S2E and S2F), and males exhibited aggression and typical nuptial coloration (Figure 4C). Additionally, gonad size, a sensitive indicator of androgen levels, is normal in these mutants (Figures 4D and 4E), indicating that these mutations do not affect masculinization. To determine whether these cells were rendered unresponsive to their preferred ligands, we exposed *trpc2b*$^{\Delta/\Delta}$ males (n = 3 of each genotype) to a cocktail of amino acids and *cnga2b*$^{\Delta/\Delta}$ males (n = 3 of each genotype) to female-conditioned water. Although *trpc2b*$^{\Delta/\Delta}$ males did not express *fosab* mRNA in microvillous neurons following exposure to amino acids, we found numerous *fosab*$^{+}$ cells in heterozygous control siblings (Figure 4F). Likewise, water conditioned by $PGF_{2\alpha}$-injected females activated very few OSNs in the ciliated cell layer of *cnga2b*$^{\Delta/\Delta}$ males, while heterozygous sibling controls exhibited numerous *fosab*$^{+}$ cells (Figure 4G). Together, these results indicate that deletion of *trpc2b* or *cnga2b* results in a blockade of microvillous or ciliated OSN activity, respectively.

To determine which class of neurons is responsible for attraction to the female fertility signal, we tested whether *cnga2b*$^{\Delta/\Delta}$ or *trpc2b*$^{\Delta/\Delta}$ males had altered attraction to water conditioned by $PGF_{2\alpha}$-injected females. We found that *trpc2b*$^{\Delta/\Delta}$ males retain a strong attraction to the $PGF_{2\alpha}$-derived pheromone signal, similar to wild-type siblings (Figure 4H). However, *cnga2b*$^{\Delta/\Delta}$ males, unlike their heterozygous sibling controls, do not prefer water conditioned by $PGF_{2\alpha}$-injected females (Figure 4H). These findings indicate that ciliated OSNs, but not microvillous OSNs, are necessary to detect one or more attractive components of fertile female odor.

Although *cnga2b*$^{\Delta/\Delta}$ males had pigmentation and aggression typical of wild-type males, we found that females paired with these males had an elevated but variable rate of non-developing embryos in broods collected from their mouths (Figure 4L). To gain insight into this reproduction phenotype, we recorded the mating behavior of *cnga2b*$^{\Delta/\Delta}$ and control sibling males. We observed that *cnga2b*$^{\Delta/\Delta}$ males exhibit a disrupted behavior pattern in which they quiver less, peck less at the female anal fin, and reduce circling with females (Figures 4I–4K; Videos S1 and S2). Additionally, we found a strong correlation between spawning attempts and egg fertilization rates in these broods (Figure 4M), suggesting that low fertilization rates in *cnga2b*$^{\Delta/\Delta}$ males result from deficiencies in mating behavior rather than reproductive physiology (Figures 4D, 4E, and 4M). These data, combined with the reduced attraction to the odor of $PGF_{2\alpha}$-injected females, are consistent with a failure to engage with fertile females, resulting in reduced fertilization.

We next asked which receptor in ciliated OSNs detects a fertile female pheromone cue. Our previous data indicate that $PGF_{2\alpha}$ is likely metabolized to an attractive pheromone by female cichlids.[50] Because the $PGF_{2\alpha}$-sensitive receptor from zebrafish,

CellPress

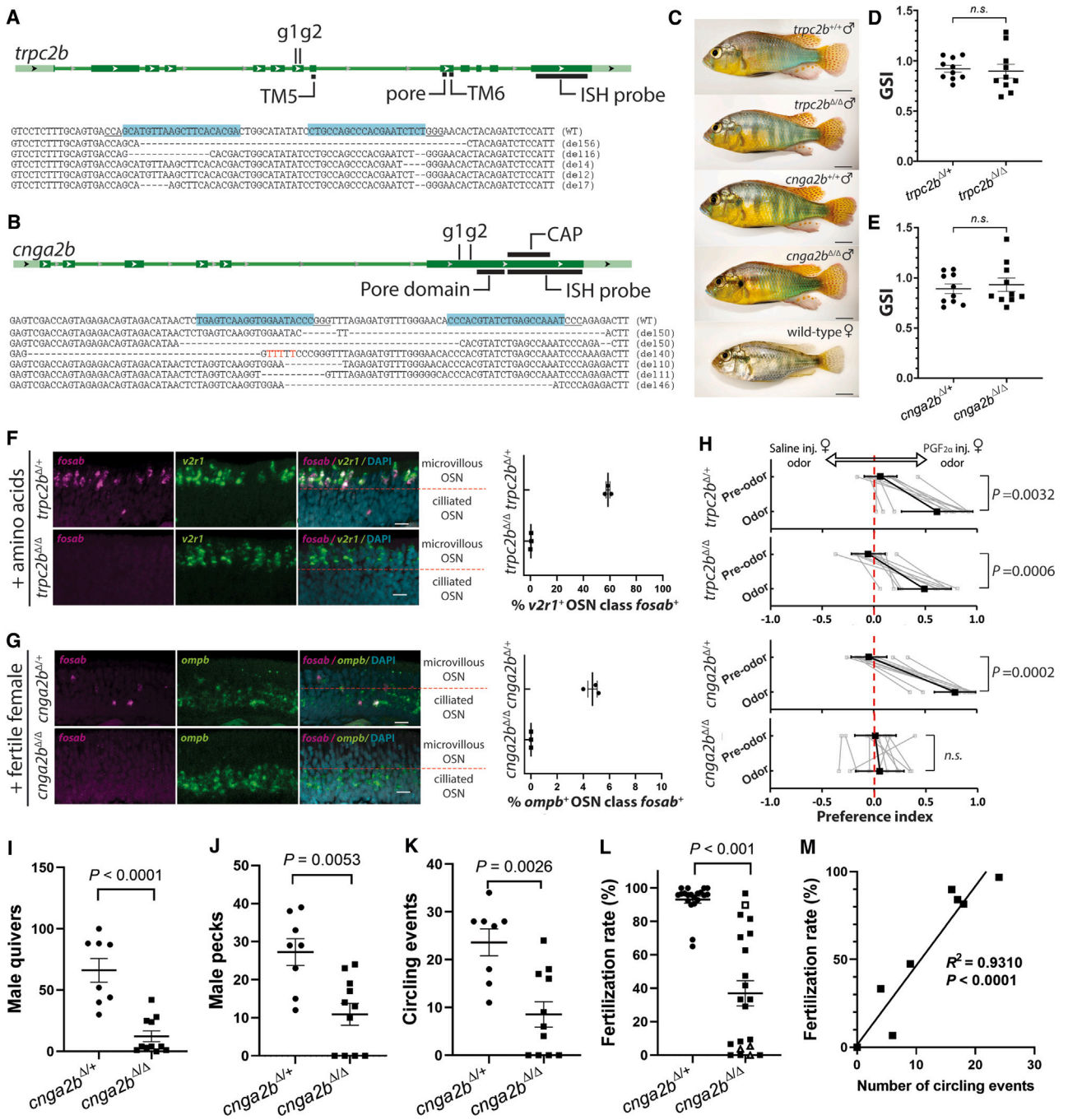


Figure 4. Deletion of OSN cellular transduction channels abolishes responses in selected sensory populations

(A) Genomic structure of *trpc2b* gene labeled for key transmembrane (TM) and ion-conducting pore.

(B) Targeting strategy for *cnga2b* gene. CAP, domain containing cAMP-binding site. g1 and g2 denote CRISPR RNA (crRNA) binding sites, highlighted in cyan; protospacer adjacent motif (PAM) sequence is underlined. CRISPR-induced mutations in animals analyzed are shown below wild-type sequence; red letters denote insertions.

(C) Male-typical morphology of *trpc2b*$^{\Delta/\Delta}$, *cnga2b*$^{\Delta/\Delta}$, and their wild-type siblings, contrasted with female. Scale bars, 1 cm.

(D and E) (D) Gonadal-somatic index (GSI) is unchanged for males with a mutation in *trpc2b* or (E) for males with a mutation in *cnga2b*. Mean ± SEM; Mann-Whitney U test, $n = 10$ fish per experiment. n.s., not significant.

(F) Amino acid mixture activates *fosab* mRNA transcription in ~60% of microvillous OSNs in *trpc2b*$^{\Delta/+}$ fish, as marked by *v2r1*$^{+}$ cells, but fails to activate *fosab* transcription in *trpc2b*$^{\Delta/\Delta}$ animals. Scale bars, 10 μm.

(legend continued on next page)

Or114, has been lost from the neoteleost lineage leading to cichlids,[50] we reasoned that a structurally similar OR may detect a $PGF_{2\alpha}$ metabolite. We therefore screened for ORs of the β subclass (the group containing *or114*) that are expressed in OSNs activated specifically by fertile females. These *A. burtoni* receptors exhibit 36%–42% identity at the amino acid level to *Danio rerio* Or114-1. We colabeled for the neural activation marker *fosab* and a pool of β OR mRNAs, and found that many β OR-expressing cells are *fosab*$^+$ following stimulation with water conditioned by fertile or $PGF_{2\alpha}$-injected females, but not non-fertile females or tank water control (Figure S4B). Subsequently we tested for expression of individual β ORs in the activated neurons and discovered that 85% of OSNs that express *or113a* were *fosab*$^+$, but almost no *or112*$^+$ or *or113b*$^+$ OSNs were activated (Figures 5A and 5B). We found that *or113a*$^+$ cells were activated by water conditioned by $PGF_{2\alpha}$-injected and fertile females, but not by males. We observed weaker activation by non-fertile females, suggesting that all females produce a moderate amount of the pheromone that activates Or113a, but its levels rise at ovulation. Additionally, we found that $PGF_{2\alpha}$, or its known metabolites, do not activate *or113a*$^+$ cells (Figures S5A and S5B), in line with our previous findings that these compounds are not attractive to male *A. burtoni*.[50] Together, these results indicate that fertile females release a novel pheromone that is sensed by Or113a.

To determine whether Or113a is necessary for male behaviors directed toward fertile females, we generated frameshift mutations in the DRY ionic lock motif of *or113a* (Figure 5C). In fish bearing biallelic mutations in *or113a*, we did not detect *or113a* transcripts in the OE (Figures S5C–S5F), consistent with the finding that mouse ORs that do not fold correctly or couple to G-proteins will fail to stabilize *OR* choice and an alternate *OR* gene will be expressed.[64–66] We tested male preference and discovered that *or113a*$^{\Delta/\Delta}$ males exhibit a weaker preference for $PGF_{2\alpha}$-injected females than do heterozygous or wild-type control siblings (Figures 5D, 5E, S7A, and S7B). This effect was found in both biallelic mutants of the F_1 and F_2 generations, indicating that this results from mutations specifically at the *or113a* locus. The contrast of this quantitative phenotype with the complete abolition of preference in *cnga2b*$^{\Delta/\Delta}$ males indicates that Or113a signaling acts in concert with additional receptors expressed in ciliated neurons to detect fertile females.

To determine whether this altered preference results in changes in reproductive behaviors, we allowed a male to interact with an ovulated wild-type female and quantified male behaviors (Figure 5F). We found that during spawning encounters, *or113a*$^{\Delta/\Delta}$ males display fewer courtship quivers (Figure 5G) and enter the spawning site fewer times (Figure 5I). Other aspects of spawning behavior were also reduced, including circling (Figure 5H), pecking (Figure 5J), and time spent in the spawning site (Figure S7C). In principal-component analysis (PCA), wild-type and mutant males can be mostly separated by the top two principal components (PCs). The most strongly loaded behavior on these PCs is the same suite of behaviors (i.e., quivers, spawning site entries, pecks, and circling) in which we find significant differences when testing individually (Figure S7F). When we calculated the probabilities of transitions between reproductive behaviors, we found that the likelihood of behaviors that followed courtship quivers was not reduced in *or113a*$^{\Delta/\Delta}$ males. This is consistent with a model in which Or113a senses a female fertility pheromone, but once courtship is initiated, subsequent reproductive behaviors do not require this receptor (Figure S7I). Although *or113a*$^{\Delta/\Delta}$ males exhibit deficiency in courtship, leading to an overall reduction in number of other mating behaviors, this does not diminish their ability to fertilize eggs (Figure S7E).

Olfactory control of parental behavior

To our surprise, we found that *cnga2b*$^{\Delta/\Delta}$ and *or113a*$^{\Delta/\Delta}$ males would occasionally collect eggs during spawning and carry these eggs for ≥10 days, in a manner similar to females (Figures 6A–6D). Healthy cichlid fry were collected from males at this time point, indicating that the motor control of mouthbrooding is intact in males. No haplochromine cichlid species (i.e., the ~1,000 species most closely related to *A. burtoni*) exhibit male mouthbrooding behavior.[67,68] We established continuous video recordings of *cnga2b*$^{\Delta/\Delta}$ and control sibling males and analyzed behavior in the hour surrounding egg laying by wild-type females. We observed that about 50% of *cnga2b*$^{\Delta/\Delta}$ males retrieve eggs during mating (Figure 6E) and some of them continue mouthbrooding eggs for days (Figure 4L), while this behavior was never observed in control *cnga2b*$^{\Delta/+}$ siblings, nor had we ever observed this behavior in wild-type males or in our other CRISPR mutant lines (n = 13 genes). Thus, our data indicate that olfactory signaling through ciliated OSNs inhibits male retrieval of eggs during spawning.

Because fertile females release a ligand that activates *or113a*$^+$ OSNs, we asked whether this receptor mediates inhibition of male mouthbrooding behavior. We found one *or113a*$^{\Delta/\Delta}$ male that performed long-term mouthbrooding care (Figure 6D; 1 out of 12 males), during which it held eggs for 12 days, and another that retrieved eggs during spawning with females (Figure S7D). However, during natural spawning, females very rapidly collect eggs, and those males that collected eggs only did so when the eggs were dispersed and females did not collect them. We therefore designed an artificial assay to allow us to control interactions with eggs during spawning, in which we

(G) Fertile female-conditioned water activates *fosab* mRNA transcription in ~5% of ciliated OSNs in *cnga2b*$^{\Delta/+}$ fish, as marked by *ompb*$^+$ cells, but fails to activate *fosab* transcription in *cnga2b*$^{\Delta/\Delta}$ animals.
(H) *trpc2b*$^{\Delta/+}$ and *trpc2b*$^{\Delta/\Delta}$ males each prefer water conditioned by $PGF_{2\alpha}$-injected females over saline-injected females. *cnga2b*$^{\Delta/+}$ males prefer water conditioned by $PGF_{2\alpha}$-injected over saline-injected females, but *cnga2b*$^{\Delta/\Delta}$ males do not exhibit a preference. Gray squares and lines represent preference index in individual trials, while black squares and lines represent mean ± SD. Mann-Whitney U test, n = 10 fish per experiment. n.s., not significant.
(I–K) Behavior in *cnga2b*$^{\Delta/\Delta}$ and *cnga2b*$^{\Delta/+}$ males was recorded with naturally fertile females. Compared with *cnga2b*$^{\Delta/+}$ male siblings, (I) *cnga2b*$^{\Delta/\Delta}$ males exhibit fewer quivers, (J) fewer pecks, and (K) less circling. n = 8–11 males per genotype. Mean ± SEM; Mann-Whitney U test.
(L) Fertilization rate by *cnga2b*$^{\Delta/\Delta}$ males is reduced compared with wild type. Open square indicates eggs mouthbrooded by *cnga2b*$^{\Delta/\Delta}$ male; closed squares indicate *cnga2b*$^{\Delta/\Delta}$ male × *cnga2b*$^{\Delta/\Delta}$ female cross; open triangles indicate *cnga2b*$^{\Delta/\Delta}$ male × wild-type female cross. Mean ± SEM; Mann-Whitney U test.
(M) Egg fertilization rates are positively correlated with number of circling events by *cnga2b*$^{\Delta/\Delta}$ males. Simple linear regression F test, b = 4.517, $F_{1,9}$ = 121.4.
See also Figures S3 and S4, Table S2, and Videos S1 and S2.

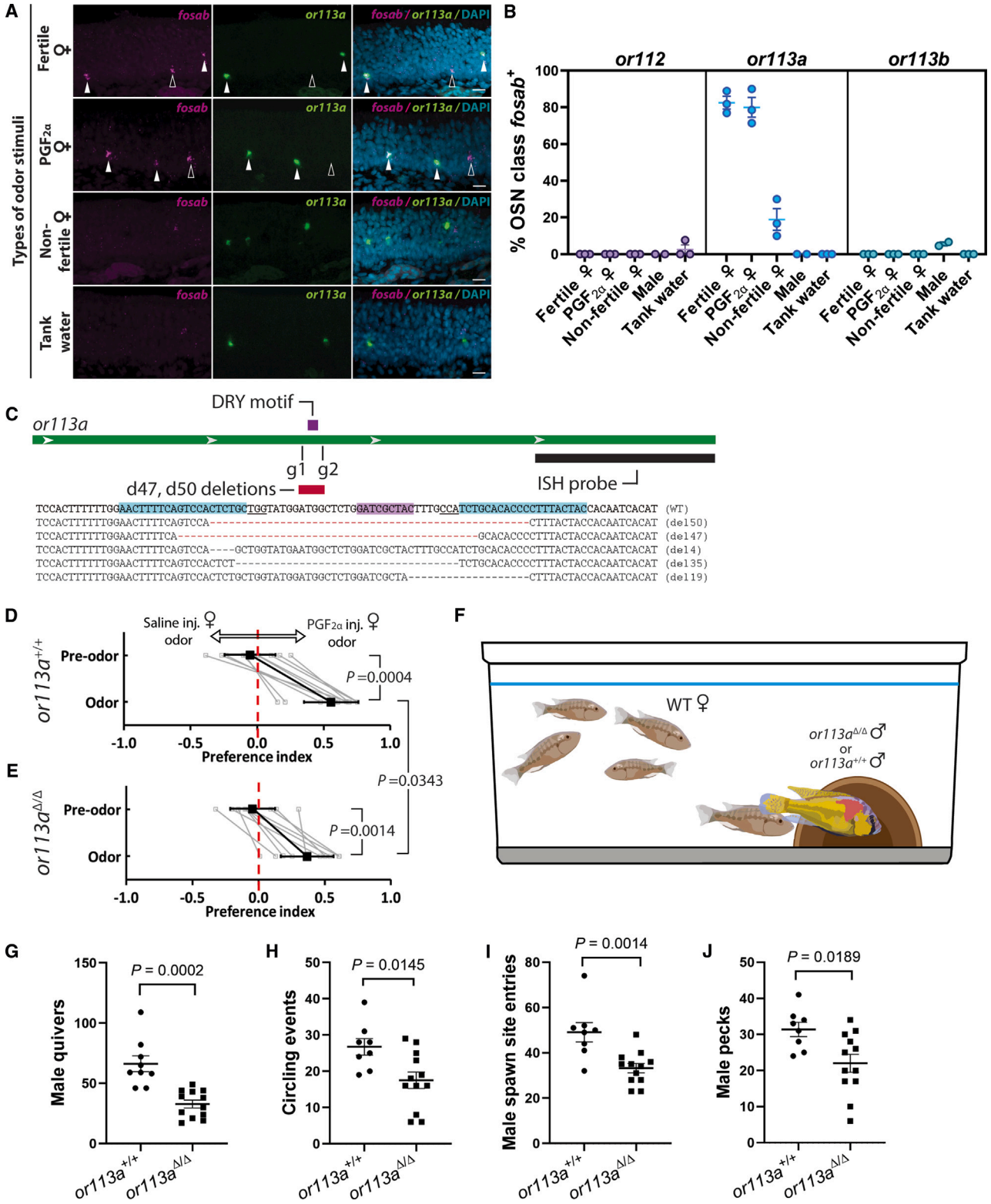


Figure 5. Fertile female cue produced in response to $PGF_{2\alpha}$ attracts males via *or113a*$^+$ sensory neurons

(A) *fosab* and *or113a* mRNA are co-expressed in olfactory epithelium following exposure to water containing female fertility cue. White arrowheads indicate the neurons co-expressing *or113a* and *fosab*. Open arrowheads indicate the neurons expressed *fosab* but not *or113a*. Scale bars, 10 μm.

(B) Quantification of *fosab* mRNA expression in *or113a*$^+$ cells following exposure to social odors.

(legend continued on next page)

released fertilized eggs during fictive spawning induced by $PGF_{2\alpha}$ injection into non-fertile females (Figure 6F). Although *or113*$^{\Delta/\Delta}$ males exhibited less courtship than wild-type siblings, they still attempt to spawn (Figures 6G and 6H). During these interactions, fictively spawning females do not collect the dispersed eggs as rapidly, giving males an opportunity to retrieve eggs. In contrast to wild-type males that mostly ignored eggs, we found that all *or113*$^{\Delta/\Delta}$ males either mouthed eggs or picked them up (Figures 6I–6K, S7G, and S7H; Videos S3 and S4). We noticed that only about 30% of *or113*$^{\Delta/\Delta}$ males continued to mouthbrood eggs for at least 45–60 min (Figure 6L), indicating that additional pathways may contribute to the continued mouthbrooding behavior in males. These results suggest a model in which a pheromonal $PGF_{2\alpha}$ metabolite produced by fertile females attracts males via Or113a and causes avoidance of egg retrieval (Figure 6M).

DISCUSSION

An outstanding question in the field of sensory biology is how ORs co-evolved with ligands. Cichlids use olfactory cues to differentiate between closely related species.[4] As cichlids represent the most explosive vertebrate species radiation,[33] variation in olfactory sensitivity or processing could alter mate choice preference and establish species barriers. Previous work in teleost fish has linked only one naturally occurring pheromone receptor, zebrafish *or114-1*, with a loss-of-function phenotype.[47] As the ability of $PGF_{2\alpha}$ to convey female fertility is not conserved across all fish species, it is important to determine how taxon-specific sensory mechanisms have replaced Or114 signaling.[50] We identify cichlid Or113a as an alternative receptor that detects a $PGF_{2\alpha}$-initiated fertility signal. Although evolution of Or114 and Or113a can explain preference for females from broad taxonomic groups (i.e., otophysans vs. neoteleostei), further specificity is required to differentiate more closely related species. Such a preference could arise from additional sensors that detect species-specific cues or fine-tuning of ligand specificity among a subset of ORs, including β-class ORs. The recent structural determination of an OR reveals the residues contained in the odorant binding region and those that determine ligand selectivity.[69] Future structure-function studies will reveal how OR sequences evolve to accommodate alternative ligands. The identification of a ligand for this receptor will provide the first opportunity to trace the shifts in pheromone sensitivity for any OR. Although our data fit with a model where $PGF_{2\alpha}$ is metabolized into a pheromone(s), it is also possible that it complexes with an excreted carrier molecule or binds a (non-Ptgfr) receptor within a female to effect the release of another pheromone.[50] Bile acids are attractive cues among cichlids, and a recent report indicates that cholic acid and taurocholic acid are produced at higher levels in fertile females.[70] These molecules have been shown to activate V1R-class receptors,[71] indicating that this is not a likely ligand for a β OR-like Or113a. However, fertility-induced bile acid production could be responsible for attraction through a parallel, Cnga2b-dependent pathway, explaining residual attraction in *or113a*$^{\Delta/\Delta}$ males.

This dual function of a pheromone receptor in attraction and parenting is reminiscent of Or67d in *Drosophila melanogaster*, which senses the male pheromone *cis*-vaccenyl acetate (cVA). This signal promotes aggression toward other males, but also inhibits courtship toward previously mated females.[72,73] Similarly, ESP1 is a male pheromone in *Mus musculus* that promotes aggression in males and receptivity in females via its receptor V2Rp5.[74,75] Or113a also regulates two distinct reproductive behaviors in the course of a reproductive interaction, enhancing two facets of sexual selection. First, Or113a enables males to invest the most effort in courting females that are fertile. Second, for a species like *A. burtoni* with a lek-like mating system where a minority of males dominate mating and partners are readily available,[76] sexual selection will favor males that sire many broods. As the major energetic investment in parenting is likely to dramatically diminish body condition and mating success,[77] males that avoid parenting would be favored.

Does altered Or113a function during evolution of cichlids explain the gain or loss of mouthbrooding behavior? The *or113a* and *or113b* paralogs emerged ~100 mya in a percomorph species (Figure S6), significantly predating the emergence of cichlid mouthbrooding behavior ~20 mya.[68] Thus, we speculate that Or113a initially detected the reproductive status of females, and this information was later co-opted to modify male cichlid behavior by causing egg avoidance. As this receptor detects a female fertility signal present during spawning, it was ideal to also inhibit mouthbrooding. Further studies of *or113a* gene orthologs across cichlid species with varying parental strategies may provide further support for olfactory control of parenting. Among cichlids, the blackchin tilapia (*Sarotherodon melanotheron*) is one of very few species that has males that have been demonstrated to initiate mouthbrooding.[67,78] We remapped genome sequencing data from *S. melanotheron*[79] and its congener, the mango tilapia, *S. galileus*,[80] and discovered a likely loss-of-function mutation in the DRY motif of Or113a in *S. melanotheron* but not in its closest, maternal caregiving relatives (Figure S8). This mutation is not fixed, suggesting that *or113a* loss of function is not responsible for the paternal phenotype in *S. melanotheron*, but is consistent with reduced purifying selection following a switch to paternal care. Prior work in *S. galileus* has indicated that there are energetic and mating opportunity costs to male mouthbrooding.[81] The relative costs to

(C) Coding region schematic for *or113a*, showing the location of CRISPR-induced mutations near DRY ionic lock motif (bases in purple) and ISH probe location. Cyan, CRISPR RNA (crRNA) binding sites; protospacer adjacent motif (PAM) sequence underlined. CRISPR-induced *or113a* mutations in animals analyzed are shown below wild-type sequence.
(D and E) (D) *or113a*$^{+/+}$ and (E) *or113a*$^{\Delta/\Delta}$ males each prefer water conditioned by $PGF_{2\alpha}$-injected females over saline-injected females. However, *or113a*$^{\Delta/\Delta}$ males have reduced preference index compared with *or113a*$^{+/+}$ male siblings. Gray squares and lines represent preference index in individual trials, while black squares and lines represent mean ± SD. Mann-Whitney U test, n = 10 fish per experiment.
(F) Behavior in *or113a*$^{\Delta/\Delta}$ and *or113a*$^{+/+}$ males was tested with naturally fertile wild-type females.
(G–J) *or113a*$^{\Delta/\Delta}$ males exhibit (G) fewer quivers, (H) less circling, (I) fewer spawn site entries, and (J) fewer pecks. n = 9–12 males per genotype. Mean ± SEM; Mann-Whitney U test.
See also Figures S4–S7 and Videos S1 and S2.

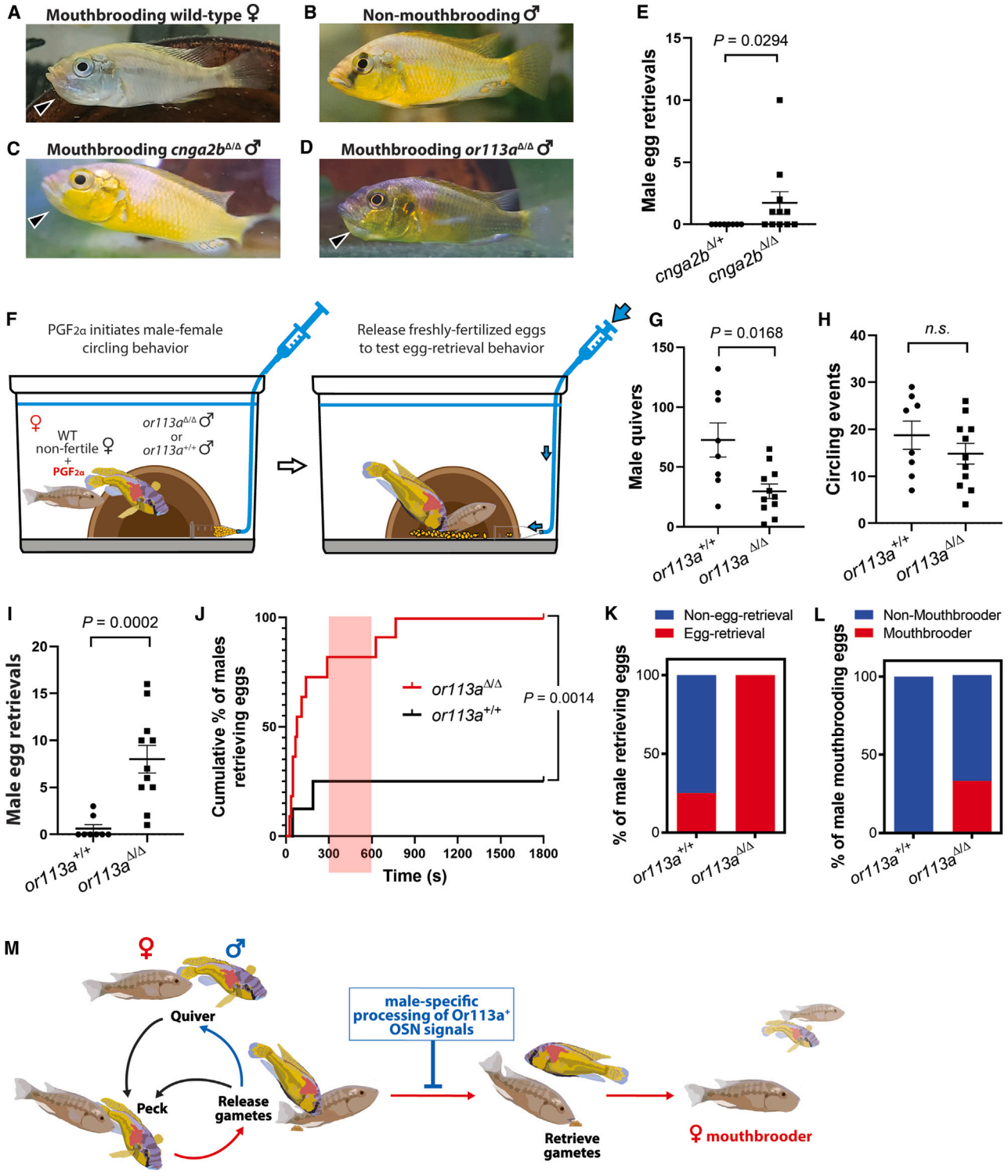


Figure 6. Or113a senses $PGF_{2\alpha}$-initiated pheromonal cue(s) that inhibit male egg retrieval

(A) Mouthbrooding wild-type female.

(B) Non-mouthbrooding male.

(C) Mouthbrooding *cnga2b*$^{\Delta/\Delta}$ male.

(D) Mouthbrooding *or113a*$^{\Delta/\Delta}$ male. Arrowheads denote distended jaw due to presence of eggs or fry.

(E) In natural spawning events, *cnga2b*$^{\Delta/\Delta}$ males frequently retrieve eggs during mating.

(legend continued on next page)

males and females are predicted to influence the change in parenting strategy. We speculate that in an ancestral cichlid with a female-skewed operational sex ratio, the Or113a signaling pathway used during attraction to fertile females was co-opted for male avoidance of mouthbrooding. High levels of sexual selection likely facilitated this behavioral change, as dominant males could monopolize more mating opportunities when they do not provide parental care.[82,83]

Our data indicate that Or113a senses a fertility pheromone, but that other receptors also regulate attraction and mouthbrooding avoidance. Although *or113a* and *cnga2b* mutant males retrieve eggs, they only occasionally brood them for more than a day, indicating that additional sensory and/or hormonal factors regulate the extent of parental behavior. As *S. melanotheron* exhibits aspects of behavioral sex role reversal,[84] it is possible that gain of paternal care results from altered sex hormone signaling pathways in, or downstream of, *or113a*$^{+}$ OSNs. Interestingly, *or113a* deletion has a sex-specific effect, as wild-type females express this gene (Figure S5D) but do not avoid mouthbrooding. Furthermore, while *or113a* mutant males initiate mouthbrooding, only a minority of males continue to hold embryos for an extended period of time, whereas females uniformly hold embryos for ~2 weeks. These results suggest that one or more sex-specific factors act either during development or around the time of spawning to promote mouthbrooding in females, despite the presence of Or113a (Figure 6M).

Our finding of a sensor that inhibits parenting in males is reminiscent of olfactory control of parental care in rodents. Virgin female rats typically ignore pups until they spend ~1 week with them, but surgical interruption of these vomeronasal and main olfactory sensory inputs causes onset of parental care within 1–2 days.[85] In mice, vomeronasal receptors detect cues present on pups and enhance pup-directed aggression by males.[86] Inhibition of signals from these receptors is essential to allow parental care, but chemosensory receptors that directly promote parental care in mice remain elusive. To our knowledge, our results are the first demonstration of a manipulation of a single chemosensory receptor that enhances parental behavior. Taken together with our findings, these data imply that olfactory signals inhibit parental care across vertebrate species. However, these manipulations also reveal—as in mammals[5,7]—that the circuits to perform parental behaviors are present in both males and females. Other known regulators of parental behavior with sex differences in levels include circulating factors like prolactin and gonadal steroid hormones; these could act on sensory epithelia or the brain to modify behavior.[87,88] Further work will reveal whether neurons that express such genes as galanin or the prolactin receptor might control cichlid parenting in a sexually dimorphic manner.[31,38,89–91] Previous work in mice has indicated that circuits for sex-specific behaviors may coexist in the brain, but their activation is limited to one sex due to dimorphic sensory systems.[7] Further study of cichlids carrying mutations at sex-determining loci and in hormone signaling[92–94] will enable a mechanistic understanding of the intersection of olfactory inputs and parenting control mechanisms. The cichlid family is rich with diversity in parental care strategies,[67,95,96] providing ample opportunities to link genetic changes with behavior evolution. Future experiments comparing cichlid species will identify the neural loci modified during the behavioral change to paternal care. Our identification of a defined olfactory input that regulates this sexually dimorphic behavior provides an entry point to understand the evolution of reproductive behaviors.

STAR★METHODS

Detailed methods are provided in the online version of this paper and include the following:

- KEY RESOURCES TABLE
- RESOURCE AVAILABILITY
  - Lead contact
  - Materials availability
  - Data and code availability
- EXPERIMENTAL MODEL AND STUDY PARTICIPANT DETAILS
- METHOD DETAILS
  - Olfactory preference test
  - Behavioral tracking and assessing preference
  - Analysis in behavior transitional probabilities
  - Fictive spawning assay
  - Tissue collection and preparation for in situ hybridization (ISH)
  - Chromogenic and dual-label fluorescence ISH
  - Single nucleus RNA-seq of the cichlid olfactory epithelium
  - Single nuclei sample quality controls
  - 10X Genomics barcoding, library preparation, and sequencing
  - Read alignment, UMI counting, and cell-calling
  - Multiple nuclei identification
  - Quality controls, data normalization, and scaling
  - Dimensionality reduction and cell clustering
  - Differential gene expression analysis
  - Gene set enrichment analysis
  - Identification of sensory transduction genes in OSNs
  - CRISPR gene targeting

(F) Schematic of artificial spawning assay to test egg-retrieval behavior during $PGF_{2\alpha}$-induced fictive spawning. Wild-type female is paired with male immediately following $PGF_{2\alpha}$ injection. Fertilized eggs from a separate female are released during circling.
(G–I) Compared with *or113a*$^{+/+}$ sibling males, *or113a*$^{\Delta/\Delta}$ males exhibit (G) fewer quivers, (H) less circling, but (I) more egg retrievals. n = 8–11 males per genotype. Mean ± SEM; Mann-Whitney U test. n.s., not significant.
(J) Males carrying biallelic mutations in *or113a* rapidly pick up eggs, while wild-type sibling males rarely retrieve eggs and do so with longer latency. 1st batch of eggs were released during circling, at time zero. 2nd batch of eggs released during red shaded interval. n = 8–11 males per genotype; log-rank (Mantel-Cox) test compares latency.
(K) During artificial spawning assay, all *or113a*$^{\Delta/\Delta}$ males exhibit egg-retrieval behavior, while only 25% of *or113a*$^{+/+}$ sibling males retrieve eggs.
(L) About 30% of *or113a*$^{\Delta/\Delta}$ males continue mouthbrooding eggs till the end of the assay (~60 min after the assay), while no *or113a*$^{+/+}$ sibling male does so.
(M) Model for olfactory control of sexually dimorphic parental care. Cichlid courtship consists of male quivering and mutual pecking, followed by gamete release. Females retrieve fertilized eggs (red arrow), while males return to courtship behavior (blue arrow). Information from *or113a*$^{+}$, *cnga2b*$^{+}$ OSNs is processed in a sexually dimorphic manner to inhibit egg retrieval in males. Among wild-type cichlids, only females provide mouthbrooding care, while males court additional females after mating.
See also Figures S7 and S8 and Videos S3 and S4.

- Behavior recordings of *cnga2b*$^{\Delta/\Delta}$ male reproduction
- Barcode sequencing for genotype mutant lines
- *Sarotherodon melanotheron* genome sequencing and comparative proteomics

- QUANTIFICATION AND STATISTICAL ANALYSIS

SUPPLEMENTAL INFORMATION

Supplemental information can be found online at https://doi.org/10.1016/j.cub.2024.07.029.

ACKNOWLEDGMENTS

We thank the Juntti, Kocher, Carleton, and Angueyra labs for valuable feedback throughout this project and the Single-Cell Ninjas, J. Tollkuhn and B. Gegenhuber, and C. Speer for discussions and resources for snRNA-seq experiments. Part of this work was conducted at the Brain & Behavior Institute – Advanced Genomic Technologies Core (BBI-AGTC), which is supported by the BBI and the University of Maryland, College Park. We acknowledge the Imaging Core Facility in the Department of Cell Biology and Molecular Genetics at the University of Maryland, College Park, for providing the Leica SP5 X confocal microscope and assistance with the imaging process. E. Taksey, M. Castanzo, and Y. Usui provided assistance with behavioral analysis and genotyping. This work was supported by National Science Foundation grant IOS-1825723 (S.A.J.), National Institutes of Health grant R35GM142872 (S.A.J.), National Institutes of Health grant DP2MH125812 (T.A.A.), and the William J. Higgins endowment (S.A.J.).

AUTHOR CONTRIBUTIONS

C.-Y.L., J.M.B., and S.A.J. designed and conceptualized the project. C.-Y.L., J.M.B., P.J., and C.J.A. conducted experiments and collected data. C.-Y.L., J.M.B., T.A.A., K.A.B., P.J., C.J.A., and S.A.J. performed data analysis. Visualization efforts were led by C.-Y.L., J.M.B., and S.A.J. S.A.J. supervised and acquired funding for the project. C.-Y.L., J.M.B., and S.A.J. wrote the original draft of the manuscript. All authors, including C.-Y.L., J.M.B., T.A.A., K.A.B., P.J., C.J.A., and S.A.J. contributed to the review and editing process.

DECLARATION OF INTERESTS

The authors declare no competing interests.

Received: March 8, 2024
Revised: May 24, 2024
Accepted: July 3, 2024
Published: August 1, 2024

REFERENCES

1. Karlson, P., and Lüscher, M. (1959). 'Pheromones': a New Term for a Class of Biologically Active Substances. Nature *183*, 55–56. https://doi.org/10.1038/183055a0.
2. Lévy, F., Keller, M., and Poindron, P. (2004). Olfactory regulation of maternal behavior in mammals. Horm. Behav. *46*, 284–302. https://doi.org/10.1016/j.yhbeh.2004.02.005.
3. Ziegler, A.B., Berthelot-Grosjean, M., and Grosjean, Y. (2013). The smell of love in Drosophila. Front. Physiol. *4*, 72. https://doi.org/10.3389/fphys.2013.00072.
4. Plenderleith, M., van Oosterhout, C., Robinson, R.L., and Turner, G.F. (2005). Female preference for conspecific males based on olfactory cues in a Lake Malawi cichlid fish. Biol. Lett. *1*, 411–414. https://doi.org/10.1098/rsbl.2005.0355.
5. Beach, F.A. (1947). A review of physiological and psychological studies of sexual behavior in mammals. Physiol. Rev. *27*, 240–307. https://doi.org/10.1152/physrev.1947.27.2.240.
6. Newman, S.W. (1999). The medial extended amygdala in male reproductive behavior. A node in the mammalian social behavior network. Ann. N. Y. Acad. Sci. *877*, 242–257. https://doi.org/10.1111/j.1749-6632.1999.tb09271.x.
7. Kimchi, T., Xu, J., and Dulac, C. (2007). A functional circuit underlying male sexual behaviour in the female mouse brain. Nature *448*, 1009–1014. https://doi.org/10.1038/nature06089.
8. Kohl, J. (2020). Parenting — a paradigm for investigating the neural circuit basis of behavior. Curr. Opin. Neurobiol. *60*, 84–91. https://doi.org/10.1016/j.conb.2019.11.011.
9. Coleman, R.T., Morantte, I., Koreman, G.T., Cheng, M.L., Ding, Y., and Ruta, V. (2023). A modular circuit architecture coordinates the diversification of courtship strategies in Drosophila. Preprint at bioRxiv. https://doi.org/10.1101/2023.09.16.558080.
10. Bendesky, A., Kwon, Y.-M., Lassance, J.-M., Lewarch, C.L., Yao, S., Peterson, B.K., He, M.X., Dulac, C., and Hoekstra, H.E. (2017). The genetic basis of parental care evolution in monogamous mice. Nature *544*, 434–439. https://doi.org/10.1038/nature22074.
11. Dulac, C., O'Connell, L.A., and Wu, Z. (2014). Neural control of maternal and paternal behaviors. Science *345*, 765–770. https://doi.org/10.1126/science.1253291.
12. Gross, M.R., and Sargent, R.C. (1985). The Evolution of Male and Female Parental Care in Fishes. Am. Zool. *25*, 807–822. https://doi.org/10.1093/icb/25.3.807.
13. Balshine, S. (2012). Patterns of parental care in vertebrates. In The Evolution of Parental Care, M. Kölliker, N.J. Royle, and P.T. Smiseth, eds. (Oxford University Press), pp. 62–80. https://doi.org/10.1093/acprof:oso/9780199692576.003.0004.
14. Fischer, E.K., Nowicki, J.P., and O'Connell, L.A. (2019). Evolution of affiliation: patterns of convergence from genomes to behaviour. Philos. Trans. R. Soc. Lond. B Biol. Sci. *374*, 20180242. https://doi.org/10.1098/rstb.2018.0242.
15. Clutton-Brock, T.H., and Harvey, P.H. (1978). Mammals, resources and reproductive strategies. Nature *273*, 191–195. https://doi.org/10.1038/273191a0.
16. Kleszczyńska, A., Sokołowska, E., and Kulczykowska, E. (2012). Variation in brain arginine vasotocin (AVT) and isotocin (IT) levels with reproductive stage and social status in males of three-spined stickleback (*Gasterosteus aculeatus*). Gen. Comp. Endocrinol. *175*, 290–296. https://doi.org/10.1016/j.ygcen.2011.11.022.
17. Partridge, C.G., MacManes, M.D., Knapp, R., and Neff, B.D. (2016). Brain Transcriptional Profiles of Male Alternative Reproductive Tactics and Females in Bluegill Sunfish. PLoS One *11*, e0167509. https://doi.org/10.1371/journal.pone.0167509.
18. Cunha, A.A.P., Partridge, C.G., Knapp, R., and Neff, B.D. (2019). Androgen and prolactin manipulation induces changes in aggressive and nurturing behavior in a fish with male parental care. Horm. Behav. *116*, 104582. https://doi.org/10.1016/j.yhbeh.2019.104582.
19. Tripp, J.A., Salas-Allende, I., Makowski, A., and Bass, A.H. (2020). Mating Behavioral Function of Preoptic Galanin Neurons is shared between Fish with Alternative Male Reproductive Tactics and Tetrapods. J. Neurosci. *40*, 1549–1559. https://doi.org/10.1523/JNEUROSCI.1276-19.2019.
20. Kindler, P.M., Bahr, J.M., Gross, M.R., and Philipp, D.P. (1991). Hormonal Regulation of Parental Care Behavior in Nesting Male Bluegills: Do the Effects of Bromocriptine Suggest a Role for Prolactin? Physiol. Zool. *64*, 310–322. https://doi.org/10.1086/physzool.64.1.30158526.
21. Hoar, W.S. (1962). Hormones and the reproductive behaviour of the male three-spined stickleback (*Gasterosteus aculeatus*). Anim. Behav. *10*, 247–266. https://doi.org/10.1016/0003-3472(62)90049-0.
22. Rodgers, E.W., Earley, R.L., and Grober, M.S. (2006). Elevated 11-ketotestosterone during paternal behavior in the Bluebanded goby (*Lythrypnus dalli*). Horm. Behav. *49*, 610–614. https://doi.org/10.1016/j.yhbeh.2006.01.008.
23. Gonçalves, D., Costa, S.S., Teles, M.C., Silva, H., Inglês, M., and Oliveira, R.F. (2014). Oestradiol and prostaglandin F2α regulate sexual displays in

females of a sex-role reversed fish. Proc. Biol. Sci. *281*, 20133070. https://doi.org/10.1098/rspb.2013.3070.

24. Carneiro, L.A., Oliveira, R.F., Canário, A.V.M., and Grober, M.S. (2003). The effect of arginine vasotocin on courtship behaviour in a blenniid fish with alternative reproductive tactics. Fish Physiol. Biochem. *28*, 241–243. https://doi.org/10.1023/B:FISH.0000030542.31395.8a.
25. Páll, M., Mayer, I., and Borg, B. (2004). Hormonal Control of Male Reproductive Behaviour in Fishes: A Stickleback Perspective. Behaviour *141*, 1499–1510. https://doi.org/10.1163/1568539042948141.
26. Bester-Meredith, J.K., and Marler, C.A. (2003). Vasopressin and the transmission of paternal behavior across generations in mated, cross-fostered Peromyscus mice. Behav. Neurosci. *117*, 455–463. https://doi.org/10.1037/0735-7044.117.3.455.
27. Stowers, L., Holy, T.E., Meister, M., Dulac, C., and Koentges, G. (2002). Loss of Sex Discrimination and Male-Male Aggression in Mice Deficient for TRP2. Science *295*, 1493–1500. https://doi.org/10.1126/science.1069259.
28. Leypold, B.G., Yu, C.R., Leinders-Zufall, T., Kim, M.M., Zufall, F., and Axel, R. (2002). Altered sexual and social behaviors in trp2 mutant mice. Proc. Natl. Acad. Sci. USA *99*, 6376–6381. https://doi.org/10.1073/pnas.082127599.
29. Mandiyan, V.S., Coats, J.K., and Shah, N.M. (2005). Deficits in sexual and aggressive behaviors in Cnga2 mutant mice. Nat. Neurosci. *8*, 1660–1662. https://doi.org/10.1038/nn1589.
30. Yoon, H., Enquist, L.W., and Dulac, C. (2005). Olfactory inputs to hypothalamic neurons controlling reproduction and fertility. Cell *123*, 669–682. https://doi.org/10.1016/j.cell.2005.08.039.
31. Wu, Z., Autry, A.E., Bergan, J.F., Watabe-Uchida, M., and Dulac, C.G. (2014). Galanin neurons in the medial preoptic area govern parental behaviour. Nature *509*, 325–330. https://doi.org/10.1038/nature13307.
32. Kocher, T.D. (2004). Adaptive evolution and explosive speciation: the cichlid fish model. Nat. Rev. Genet. *5*, 288–298. https://doi.org/10.1038/nrg1316.
33. Salzburger, W. (2018). Understanding explosive diversification through cichlid fish genomics. Nat. Rev. Genet. *19*, 705–717. https://doi.org/10.1038/s41576-018-0043-9.
34. Fujimura, K., and Kocher, T.D. (2011). Tol2-mediated transgenesis in tilapia (Oreochromis niloticus). Aquaculture *319*, 342–346. https://doi.org/10.1016/j.aquaculture.2011.07.021.
35. Juntti, S.A., Hu, C.K., and Fernald, R.D. (2013). Tol2-Mediated Generation of a Transgenic Haplochromine Cichlid, Astatotilapia burtoni. PLoS One *8*, e77647. https://doi.org/10.1371/journal.pone.0077647.
36. Li, M., Yang, H., Zhao, J., Fang, L., Shi, H., Li, M., Sun, Y., Zhang, X., Jiang, D., Zhou, L., and Wang, D. (2014). Efficient and heritable gene targeting in tilapia by CRISPR/Cas9. Genetics *197*, 591–599. https://doi.org/10.1534/genetics.114.163667.
37. Juntti, S.A., Hilliard, A.T., Kent, K.R., Kumar, A., Nguyen, A., Jimenez, M.A., Loveland, J.L., Mourrain, P., and Fernald, R.D. (2016). A Neural Basis for Control of Cichlid Female Reproductive Behavior by Prostaglandin F2α. Curr. Biol. *26*, 943–949. https://doi.org/10.1016/j.cub.2016.01.067.
38. Butler, J.M., Herath, E.M., Rimal, A., Whitlow, S.M., and Maruska, K.P. (2020). Galanin neuron activation in feeding, parental care, and infanticide in a mouthbrooding African cichlid fish. Horm. Behav. *126*, 104870. https://doi.org/10.1016/j.yhbeh.2020.104870.
39. Sorensen, P.W., and Baker, C. (2014). Species-Specific Pheromones and Their Roles in Shoaling, Migration, and Reproduction: a critical review and synthesis. In Fish Pheromones and Related Cues (Wiley), pp. 11–32. https://doi.org/10.1002/9781118794739.ch2.
40. Wyatt, T.D. (2017). Pheromones. Curr. Biol. *27*, R739–R743. https://doi.org/10.1016/j.cub.2017.06.039.
41. Beach, F.A. (1976). Sexual attractivity, proceptivity, and receptivity in female mammals. Horm. Behav. *7*, 105–138. https://doi.org/10.1016/0018-506x(76)90008-8.
42. Sorensen, P.W., Appelt, C., Stacey, N.E., Goetz, F.W., and Brash, A.R. (2018). High levels of circulating prostaglandin F2α associated with ovulation stimulate female sexual receptivity and spawning behavior in the goldfish (Carassius auratus). Gen. Comp. Endocrinol. *267*, 128–136. https://doi.org/10.1016/j.ygcen.2018.06.014.
43. Sorensen, P.W., Hara, T.J., Stacey, N.E., and Goetz, F.W. (1988). F Prostaglandins Function as Potent Olfactory Stimulants that Comprise the Postovulatory Female Sex Pheromone in Goldfish. Biol. Reprod. *39*, 1039–1050. https://doi.org/10.1095/biolreprod39.5.1039.
44. Stacey, N.E. (1976). Effects of indomethacin and prostaglandins on the spawning behaviour of female goldfish. Prostaglandins *12*, 113–126. https://doi.org/10.1016/s0090-6980(76)80010-x.
45. Kidd, M.R., Dijkstra, P.D., Alcott, C., Lavee, D., Ma, J., O'Connell, L.A., and Hofmann, H.A. (2013). Prostaglandin F2 αfacilitates female mating behavior based on male performance. Behav. Ecol. Sociobiol. *67*, 1307–1315. https://doi.org/10.1007/S00265-013-1559-9.
46. Poling, K.R., Fraser, E.J., and Sorensen, P.W. (2001). The three steroidal components of the goldfish preovulatory pheromone signal evoke different behaviors in males. Comp. Biochem. Physiol. B Biochem. Mol. Biol. *129*, 645–651. https://doi.org/10.1016/S1096-4959(01)00361-X.
47. Yabuki, Y., Koide, T., Miyasaka, N., Wakisaka, N., Masuda, M., Ohkura, M., Nakai, J., Tsuge, K., Tsuchiya, S., Sugimoto, Y., and Yoshihara, Y. (2016). Olfactory receptor for prostaglandin F2α mediates male fish courtship behavior. Nat. Neurosci. *19*, 897–904. https://doi.org/10.1038/nn.4314.
48. Cole, T.B., and Stacey, N.E. (2006). Olfactory responses to steroids in an African mouth-brooding cichlid, Haplochromis burtoni (Günther). J. Fish Biol. *68*, 661–680. https://doi.org/10.1111/j.0022-1112.2006.00944.x.
49. Murphy, C.A., Stacey, N.E., and Corkum, L.D. (2001). Putative Steroidal Pheromones in the Round Goby, Neogobius melanostomus: Olfactory and Behavioral Responses. J. Chem. Ecol. *27*, 443–470. https://doi.org/10.1023/A:1010376503197.
50. Li, C.-Y., Lawrence, K., Merlo-Coyne, J., and Juntti, S.A. (2023). Prostaglandin F2α drives female pheromone signaling in cichlids, revealing a basis for evolutionary divergence in olfactory signaling. Proc. Natl. Acad. Sci. USA *120*, e2214418120. https://doi.org/10.1073/pnas.2214418120.
51. Hughes, L.C., Ortí, G., Huang, Y., Sun, Y., Baldwin, C.C., Thompson, A.W., Arcila, D., Betancur-R, R., Li, C., Becker, L., et al. (2018). Comprehensive phylogeny of ray-finned fishes (Actinopterygii) based on transcriptomic and genomic data. Proc. Natl. Acad. Sci. USA *115*, 6249–6254. https://doi.org/10.1073/pnas.1719358115.
52. Yoshihara, Y. (2009). Molecular Genetic Dissection of the Zebrafish Olfactory System. In Chemosensory Systems in Mammals, Fishes, and Insects, *47*, S. Korsching, and W. Meyerhof, eds. (Springer), pp. 1–19. https://doi.org/10.1007/400_2008_1.
53. Bayramli, X., Kocagöz, Y., Sakizli, U., and Fuss, S.H. (2017). Patterned Arrangements of Olfactory Receptor Gene Expression in Zebrafish are Established by Radial Movement of Specified Olfactory Sensory Neurons. Sci. Rep. *7*, 5572. https://doi.org/10.1038/s41598-017-06041-1.
54. DeMaria, S., Berke, A.P., Van Name, E., Heravian, A., Ferreira, T., and Ngai, J. (2013). Role of a Ubiquitously Expressed Receptor in the Vertebrate Olfactory System. J. Neurosci. *33*, 15235–15247. https://doi.org/10.1523/JNEUROSCI.2339-13.2013.
55. Hansen, A., and Zielinski, B.S. (2005). Diversity in the olfactory epithelium of bony fishes: Development, lamellar arrangement, sensory neuron cell types and transduction components. J. Neurocytol. *34*, 183–208. https://doi.org/10.1007/s11068-005-8353-1.
56. Sato, Y., Miyasaka, N., and Yoshihara, Y. (2005). Mutually Exclusive Glomerular Innervation by Two Distinct Types of Olfactory Sensory Neurons Revealed in Transgenic Zebrafish. J. Neurosci. *25*, 4889–4897. https://doi.org/10.1523/JNEUROSCI.0679-05.2005.

57. Ahuja, G., Bozorg Nia, S., Zapilko, V., Shiriagin, V., Kowatschew, D., Oka, Y., and Korsching, S.I. (2014). Kappe neurons, a novel population of olfactory sensory neurons. Sci. Rep. *4*, 4037. https://doi.org/10.1038/srep04037.

58. Oka, Y., Saraiva, L.R., and Korsching, S.I. (2012). Crypt Neurons Express a Single V1R-Related ora Gene. Chem. Senses *37*, 219–227. https://doi.org/10.1093/chemse/bjr095.

59. Kermen, F., Franco, L.M., Wyatt, C., and Yaksi, E. (2013). Neural circuits mediating olfactory-driven behavior in fish. Front. Neural Circuits *7*, 62. https://doi.org/10.3389/fncir.2013.00062.

60. Schmachtenberg, O., and Bacigalupo, J. (2004). Olfactory transduction in ciliated receptor neurons of the Cabinza grunt, Isacia conceptionis (teleostei: haemulidae). Eur. J. Neurosci. *20*, 3378–3386. https://doi.org/10.1111/j.1460-9568.2004.03825.x.

61. Hansen, A., and Zeiske, E. (1998). The Peripheral Olfactory Organ of the Zebrafish, Danio rerio: an Ultrastructural Study. Chem. Senses *23*, 39–48. https://doi.org/10.1093/chemse/23.1.39.

62. Li, C.-Y., Steighner, J.R., Sweatt, G., Thiele, T.R., and Juntti, S.A. (2021). Manipulation of the Tyrosinase gene permits improved CRISPR/Cas editing and neural imaging in cichlid fish. Sci. Rep. *11*, 15138. https://doi.org/10.1038/s41598-021-94577-8.

63. Brunet, L.J., Gold, G.H., and Ngai, J. (1996). General Anosmia Caused by a Targeted Disruption of the Mouse Olfactory Cyclic Nucleotide–Gated Cation Channel. Neuron *17*, 681–693. https://doi.org/10.1016/S0896-6273(00)80200-7.

64. Imai, T., Suzuki, M., and Sakano, H. (2006). Odorant receptor-derived cAMP signals direct axonal targeting. Science *314*, 657–661. https://doi.org/10.1126/science.1131794.

65. Monahan, K., and Lomvardas, S. (2015). Monoallelic Expression of Olfactory Receptors. Annu. Rev. Cell Dev. Biol. *31*, 721–740. https://doi.org/10.1146/annurev-cellbio-100814-125308.

66. Ferreira, T., Wilson, S.R., Choi, Y.G., Risso, D., Dudoit, S., Speed, T.P., and Ngai, J. (2014). Silencing of Odorant Receptor Genes by G Protein $\beta\gamma$ Signaling Ensures the Expression of One Odorant Receptor per Olfactory Sensory Neuron. Neuron *81*, 847–859. https://doi.org/10.1016/j.neuron.2014.01.001.

67. Balshine, S., and Abate, M.E. (2021). Parental Care in Cichlid Fishes. In The Behavior, Ecology and Evolution of Cichlid Fishes, , M.E. Abate, and D.L.G. Noakes, eds. (Springer), pp. 541–586. https://doi.org/10.1007/978-94-024-2080-7_15.

68. Goodwin, N.B., Balshine-Earn, S., and Reynolds, J.D. (1998). Evolutionary Transitions in Parental Care in Cichlid Fish. Proc. R. Soc. Lond. B *265*, 2265–2272. https://doi.org/10.1098/rspb.1998.0569.

69. Billesbølle, C.B., de March, C.A., van der Velden, W.J.C., Ma, N., Tewari, J., del Torrent, C.L., Li, L., Faust, B., Vaidehi, N., Matsunami, H., and Manglik, A. (2023). Structural basis of odorant recognition by a human odorant receptor. Nature *615*, 742–749. https://doi.org/10.1038/s41586-023-05798-y.

70. Ashouri, S., Da Silva, J.P., Canário, A.V.M., and Hubbard, P.C. (2023). Bile acids as putative social signals in Mozambique tilapia (Oreochromis mossambicus). Physiol. Behav. *272*, 11437. https://doi.org/10.1016/j.physbeh.2023.114378.

71. Cong, X., Zheng, Q., Ren, W., Chéron, J.-B., Fiorucci, S., Wen, T., Zhang, C., Yu, H., Golebiowski, J., and Yu, Y. (2019). Zebrafish olfactory receptors ORAs differentially detect bile acids and bile salts. J. Biol. Chem. *294*, 6762–6771. https://doi.org/10.1074/jbc.RA118.006483.

72. Kurtovic, A., Widmer, A., and Dickson, B.J. (2007). A single class of olfactory neurons mediates behavioural responses to a Drosophila sex pheromone. Nature *446*, 542–546. https://doi.org/10.1038/nature05672.

73. Wang, L., and Anderson, D.J. (2010). Identification of an aggression-promoting pheromone and its receptor neurons in Drosophila. Nature *463*, 227–231. https://doi.org/10.1038/nature08678.

74. Haga, S., Hattori, T., Sato, T., Sato, K., Matsuda, S., Kobayakawa, R., Sakano, H., Yoshihara, Y., Kikusui, T., and Touhara, K. (2010). The male mouse pheromone ESP1 enhances female sexual receptive behaviour through a specific vomeronasal receptor. Nature *466*, 118–122. https://doi.org/10.1038/nature09142.

75. Itakura, T., Murata, K., Miyamichi, K., Ishii, K.K., Yoshihara, Y., and Touhara, K. (2022). A single vomeronasal receptor promotes intermale aggression through dedicated hypothalamic neurons. Neuron *110*, 2455–2469.e8. https://doi.org/10.1016/j.neuron.2022.05.002.

76. Fernald, R.D., and Hirata, N.R. (1977). Field study of Haplochromis burtoni: Quantitative behavioral observations. Anim. Behav. *25*, 964–975. https://doi.org/10.1016/0003-3472(77)90048-3.

77. O'Rourke, C.F., and Renn, S.C. (2015). Integrating adaptive trade-offs between parental care and feeding regulation. Curr. Opin. Behav. Sci. *6*, 160–167. https://doi.org/10.1016/j.cobeha.2015.11.010.

78. Aronson, L.R. (1949). An analysis of reproductive behavior in the mouth-breeding cichlid fish, Tilapia macrocephala (Bleeker). Zool. Sci. Contrib. NY Zool. Soc. *34*, 133–158.

79. Gammerdinger, W.J., Conte, M.A., Baroiller, J.-F., D'Cotta, H., and Kocher, T.D. (2016). Comparative analysis of a sex chromosome from the blackchin tilapia, Sarotherodon melanotheron. BMC Genomics *17*, 808. https://doi.org/10.1186/s12864-016-3163-7.

80. Poelstra, J.W., Richards, E.J., and Martin, C.H. (2018). Speciation in sympatry with ongoing secondary gene flow and a potential olfactory trigger in a radiation of Cameroon cichlids. Mol. Ecol. *27*, 4270–4288. https://doi.org/10.1111/mec.14784.

81. Balshine-Earn, S. (1995). The costs of parental care in Galilee St Peter's fish, Sarotherodon galilaeus. Anim. Behav. *50*, 1–7. https://doi.org/10.1006/anbe.1995.0214.

82. Balshine-Earn, S. (1997). The benefits of uniparental versus biparental mouth brooding in Galilee St. Peter's fish. J. Fish Biol. *50*, 371–381. https://doi.org/10.1111/j.1095-8649.1997.tb01365.x.

83. Keenleyside, M.H.A. (1985). Bigamy and mate choice in the biparental cichlid fish Cichlasoma nigrofasciatum. Behav. Ecol. Sociobiol. *17*, 285–290. https://doi.org/10.1007/BF00300148.

84. Balshine-Earn, S., and McAndrew, B.J. (1995). Sex-Role Reversal in the Black-Chinned Tilapia, Sarotherodon melanotheron (Rüppel) (Cichlidae). Behaviour *132*, 861–874. https://doi.org/10.1163/156853995X00045.

85. Fleming, A., Vaccarino, F., Tambosso, L., and Chee, P. (1979). Vomeronasal and Olfactory System Modulation of Maternal Behavior in the Rat. Science *203*, 372–374. https://doi.org/10.1126/science.760196.

86. Isogai, Y., Wu, Z., Love, M.I., Ahn, M.H.-Y., Bambah-Mukku, D., Hua, V., Farrell, K., and Dulac, C. (2018). Multisensory Logic of Infant-Directed Aggression by Males. Cell *175*, 1827–1841.e1. https://doi.org/10.1016/j.cell.2018.11.032.

87. Bowers, J.M., Li, C.-Y., Parker, C.G., Westbrook, M.E., and Juntti, S.A. (2023). Pheromone Perception in Fish: Mechanisms and Modulation by Internal Status. Integr. Comp. Biol. *63*, 407–427. https://doi.org/10.1093/icb/icad049.

88. Dey, S., Chamero, P., Pru, J.K., Chien, M.-S., Ibarra-Soria, X., Spencer, K.R., Logan, D.W., Matsunami, H., Peluso, J.J., and Stowers, L. (2015). Cyclic Regulation of Sensory Perception by a Female Hormone Alters Behavior. Cell *161*, 1334–1344. https://doi.org/10.1016/j.cell.2015.04.052.

89. Kohl, J., Babayan, B.M., Rubinstein, N.D., Autry, A.E., Marin-Rodriguez, B., Kapoor, V., Miyamishi, K., Zweifel, L.S., Luo, L., Uchida, N., and Dulac, C. (2018). Functional circuit architecture underlying parental behaviour. Nature *556*, 326–331. https://doi.org/10.1038/s41586-018-0027-0.

90. Smiley, K.O., Brown, R.S.E., and Grattan, D.R. (2022). Prolactin Action is Necessary for Parental Behavior in Male Mice. J. Neurosci. *42*, 8308–8327. https://doi.org/10.1523/JNEUROSCI.0558-22.2022.

91. Ammari, R., Monaca, F., Cao, M., Nassar, E., Wai, P., Del Grosso, N.A., Lee, M., Borak, N., Schneider-Luftman, D., and Kohl, J. (2023). Hormone-mediated neural remodeling orchestrates parenting onset during pregnancy. Science *382*, 76–81. https://doi.org/10.1126/science.adi0576.

92. Alward, B.A., Laud, V.A., Skalnik, C.J., York, R.A., Juntti, S.A., and Fernald, R.D. (2020). Modular genetic control of social status in a cichlid fish. Proc. Natl. Acad. Sci. USA *117*, 28167–28174. https://doi.org/10.1073/pnas.2008925117.

93. Juntti, S.A., and Fernald, R.D. (2016). Timing reproduction in teleost fish: cues and mechanisms. Curr. Opin. Neurobiol. *38*, 57–62. https://doi.org/10.1016/j.conb.2016.02.006.

94. Roberts, N.B., Juntti, S.A., Coyle, K.P., Dumont, B.L., Stanley, M.K., Ryan, A.Q., Fernald, R.D., and Roberts, R.B. (2016). Polygenic sex determination in the cichlid fish Astatotilapia burtoni. BMC Genomics *17*, 835. https://doi.org/10.1186/s12864-016-3177-1.

95. Sefc, K.M. (2011). Mating and Parental Care in Lake Tanganyika's Cichlids. Int. J. Evol. Biol. *2011*, 47087. https://doi.org/10.4061/2011/470875.

96. Kidd, M.R., Duftner, N., Koblmüller, S., Sturmbauer, C., and Hofmann, H.A. (2012). Repeated Parallel Evolution of Parental Care Strategies within Xenotilapia, a Genus of Cichlid Fishes from Lake Tanganyika. PLoS One *7*, e31236. https://doi.org/10.1371/journal.pone.0031236.

97. Pérez-Escudero, A., Vicente-Page, J., Hinz, R.C., Arganda, S., and de Polavieja, G.G. (2014). idTracker: tracking individuals in a group by automatic identification of unmarked animals. Nat. Methods *11*, 743–748. https://doi.org/10.1038/nmeth.2994.

98. Heaton, H., Talman, A.M., Knights, A., Imaz, M., Gaffney, D.J., Durbin, R., Hemberg, M., and Lawniczak, M.K.N. (2020). Souporcell: robust clustering of single-cell RNA-seq data by genotype without reference genotypes. Nat. Methods *17*, 615–620. https://doi.org/10.1038/s41592-020-0820-1.

99. Hao, Y., Hao, S., Andersen-Nissen, E., Mauck, W.M., Zheng, S., Butler, A., Lee, M.J., Wilk, A.J., Darby, C., Zager, M., et al. (2021). Integrated analysis of multimodal single-cell data. Cell *184*, 3573–3587.e29. https://doi.org/10.1016/j.cell.2021.04.048.

100. Friard, O., and Gamba, M. (2016). BORIS: a free, versatile open-source event-logging software for video/audio coding and live observations. Methods Ecol. Evol. *7*, 1325–1330. https://doi.org/10.1111/2041-210X.12584.

101. Schindelin, J., Arganda-Carreras, I., Frise, E., Kaynig, V., Longair, M., Pietzsch, T., Preibisch, S., Rueden, C., Saalfeld, S., Schmid, B., et al. (2012). Fiji: an open-source platform for biological-image analysis. Nat. Methods *9*, 676–682. https://doi.org/10.1038/nmeth.2019.

102. Martelotto, L.G., and Martelotto, L. (2020). 'Frankenstein' protocol for nuclei isolation from fresh and frozen tissue for snRNAseq V.2. protocol.io. https://doi.org/10.17504/protocols.io.3fkgjkw.

103. Tung, P.-Y., Blischak, J.D., Hsiao, C.J., Knowles, D.A., Burnett, J.E., Pritchard, J.K., and Gilad, Y. (2017). Batch effects and the effective design of single-cell gene expression studies. Sci. Rep. *7*, 39921. https://doi.org/10.1038/srep39921.

104. Zheng, G.X.Y., Terry, J.M., Belgrader, P., Ryvkin, P., Bent, Z.W., Wilson, R., Ziraldo, S.B., Wheeler, T.D., McDermott, G.P., Zhu, J., et al. (2017). Massively parallel digital transcriptional profiling of single cells. Nat. Commun. *8*, 14049. https://doi.org/10.1038/ncomms14049.

105. Lun, A.T.L., Riesenfeld, S., Andrews, T., Dao, T.P., Gomes, T., Participants in the 1st Human Cell Atlas Jamboree, and Marioni, J.C. (2019). EmptyDrops: distinguishing cells from empty droplets in droplet-based single-cell RNA sequencing data. Genome Biol. *20*, 63. https://doi.org/10.1186/s13059-019-1662-y.

106. Li, H. (2021). New strategies to improve minimap2 alignment accuracy. Bioinformatics *37*, 4572–4574. https://doi.org/10.1093/bioinformatics/btab705.

107. Li, H. (2018). Minimap2: pairwise alignment for nucleotide sequences. Bioinformatics *34*, 3094–3100. https://doi.org/10.1093/bioinformatics/bty191.

108. Garrison, E., and Marth, G. (2012). Haplotype-based variant detection from short-read sequencing. Preprint at arXiv. https://doi.org/10.48550/arXiv.1207.3907.

109. Iida, M., Suzuki, M., Sakane, Y., Nishide, H., Uchiyama, I., Yamamoto, T., Suzuki, K.T., and Fujii, S. (2020). A simple and practical workflow for genotyping of CRISPR–Cas9-based knockout phenotypes using multiplexed amplicon sequencing. Genes Cells *25*, 498–509. https://doi.org/10.1111/gtc.12775.

110. Clement, K., Rees, H., Canver, M.C., Gehrke, J.M., Farouni, R., Hsu, J.Y., Cole, M.A., Liu, D.R., Joung, J.K., Bauer, D.E., et al. (2019). CRISPResso2 provides accurate and rapid genome editing sequence analysis. Nat. Biotechnol. *37*, 224–226. https://doi.org/10.1038/s41587-019-0032-3.

111. Conte, M.A., Gammerdinger, W.J., Bartie, K.L., Penman, D.J., and Kocher, T.D. (2017). A high quality assembly of the Nile Tilapia (Oreochromis niloticus) genome reveals the structure of two sex determination regions. BMC Genomics *18*, 341. https://doi.org/10.1186/s12864-017-3723-5.

STAR★METHODS

KEY RESOURCES TABLE

REAGENT or RESOURCE	SOURCE	IDENTIFIER
Antibodies		
Anti-Digoxigenin-AP Fab fragments (sheep)	Roche	Cat# 11093274910; RRID:AB_514497
Anti-Digoxigenin-POD Fab fragments (sheep)	Roche	Cat# 11207733910; RRID:AB_514500
Anti-Fluorescein-POD Fab fragments (sheep)	Roche	Cat# 11426346910; RRID:AB_840257
Chemicals, peptides, and recombinant proteins		
Protector RNase Inhibitor	Millipore Sigma	Cat# RNAINH-RO
Nuclei EZ Prep Kit	Millipore Sigma	Cat# NUC101
TSA Fluorescein System	AKOYA	Cat# NEL701A001KT
TSA Cyanine 3 Reagent Pack	AKOYA	SAT704A001EA
TSA Cyanine 5 Reagent Pack	AKOYA	SAT705A001EA
Critical commercial assays		
Chromium Single Cell 3' Reagent Kit: GEM, Library, and Gel Bead Kit v3, 4 rxns	10X Genomics	Cat# PN-1000092
NextSeq 1000 P2 Reagents (100 Cycles) v3	Illumina	Cat# SN EC1052303-EC11
Deposited data		
ssSeq_Aburt_ofep_1; ssSeq_Aburt_ofep_2 (single nucleus RNA-seq sample)	This paper	NCBI BioSample: SAMN41491291, SAMN41491292
Code for analyzing snRNA-seq data	This paper	Zenodo: https://doi.org/10.5281/zenodo.12610716
Experimental models: Organisms/strains		
A. burtoni wild-type	Derived from Fernald lab[76]	N/A
A. burtoni cnga2b$^{\Delta/\Delta}$	This paper	N/A
A. burtoni trpc2b$^{\Delta/\Delta}$	This paper	N/A
A. burtoni or113a$^{\Delta/\Delta}$	This paper	N/A
Oligonucleotides		
Primers (see Table S2 for detailed sequences)	IDT	N/A
Guide RNAs (see Table S2 for detailed sequences)	IDT	N/A
Software and algorithms		
Cell Ranger v7	10X Genomics[97]	https://www.10xgenomics.com/support/software/cell-ranger/latest
Souporcell v2	Heaton et al.[98]	https://github.com/wheaton5/souporcell
Seurat v4.0.6	Hao et al.[99]	https://satijalab.org/seurat/articles/install_v5
Prism GraphPad	N/A	https://www.graphpad.com
BORIS	Friard and Gamba et al.[100]	https://www.boris.unito.it/
FIJI	Schindelin et al.[101]	https://fiji.sc

RESOURCE AVAILABILITY

Lead contact

Further information and requests for resources and reagents should be directed to and will be fulfilled by the lead contact, Scott Juntti (sjuntti@umd.edu).

Materials availability

All reagents and cichlid strains generated in this study are available from the lead contact upon request.

Data and code availability

Single-cell RNA-seq data have been deposited at NCBI database. Accession numbers: SAMN41491291 and SAMN41491292.

All original code has been deposited at https://github.com/jmbowers312/juntti_cichlid_scseq/tree/v1.0.0 and is publicly available as of the date of publication. DOIs are listed in the key resources table.

Any additional information required to reanalyze the data reported in this work paper is available from the lead contact upon request.

EXPERIMENTAL MODEL AND STUDY PARTICIPANT DETAILS

Mixed-sex groups of adult *A. burtoni* derived from Lake Tanganyika[76] were raised at the University of Maryland. Fish were maintained in 32- to 80-liter community tanks with pH ~8.0, 25°C water temperature, and a 12:12-h light:dark cycle with 15-min dusk and dawn periods. Gravel and terracotta pots provided substrate that facilitates the establishment and maintenance of territories for reproduction. Fish were fed daily with cichlid food pellets (Jehmco) between 0900 h and 1100 h. All animal maintenance and experimental procedures were approved by the Institutional Animal Care and Use Committee of the University of Maryland (protocol 2133862).

METHOD DETAILS

Olfactory preference test

Male olfactory preference was assessed using a dichotomous choice paradigm in a 120 liter tank which was divided into three sections by transparent, permeable acrylic dividers, as in our previous work.[50] Ten holes (2 mm diameter) on the left and right side of dividers allowed odor cues to diffuse into the central compartment. Two peristaltic pumps were set up underneath the preference tank to deliver odor cues (at ~0.3 ml/sec) from two separate 8-liter tanks into the left and right compartments. The 8-liter tanks containing either stimulus or control odors were set underneath the preference tank and covered with black curtains to prevent any visual information being revealed to the focal males. The sides of odor cues were randomly decided by flipping a coin. Two adult males (> 1 year old; standard length >5 cm) were placed in the central compartment to acclimate overnight. An additional transparent divider separated the two focal males to prevent direct physical interactions. Two opaque shelters with a transparent roof were set in the preference tank to mimic a spawning site and allow automatic tracking. *A. burtoni* is a highly social species, we therefore used two males in each preference trial to increase explorative activity in the preference tank. Focal males were acclimated in the preference tank for at least 3–16 hrs until they resumed normal activity and freely explored the tank environment. On the day of the trial, a Raspberry Pi camera (Raspberry Pi 3 Model B & Camera Module v2) recorded the behavior performance of focal males. In all trials, 90 min of "pre-odor" stage (i.e., no odor cue was delivered into the tank) was recorded to assess baseline preference. Then the pumps were turned on and another 90 min of "odor" stage (i.e., when odor cue was delivered into left and right compartments) was recorded.

To collect fertile female odors, fertile females were identified based on 1) distended abdomen, 2) territorial aggression toward other females, and 3) frequent spawning site visits. To further confirm whether the female was ready to spawn, the potential fertile female was transferred into the tank with a dominant male and was observed for 30 minutes for the display of circling behavior. One day before preference trials, one fertile female and one size-matched (standard length difference < 5 mm) non-fertile female were transferred into two 8-liter odor tanks which contained 5 liters of clean aquarium water (23 g cichlid salt (Seachem), 400 mL saturated sodium bicarbonate solution, dissolved in 150 liter of reverse osmosis water). These females were acclimated overnight (~16 hours) to accumulate odor cues in the tank. After finishing the trials, fertile females were transferred into a tank with a dominant male, and we confirmed they spawned within 24 hours.

To collect odor cues from $PGF_{2\alpha}$-injected females, 30 min prior to odor delivery, non-fertile females were identified and given an intraperitoneal injection of 1.5 μg/gram body mass of $PGF_{2\alpha}$. Another size-matched, non-fertile female received the same amount of saline as control. The $PGF_{2\alpha}$- and saline-injected females were immediately returned to the odor tanks, and odor delivery began 30 min following injection. The $PGF_{2\alpha}$ working solution (3 μg/μL) was freshly prepared before injection and the recipe was as follows: mixing 8 μL saline (0.5%), 1 μL Fast Green FCF dye (0.1%) and 1 μL of $PGF_{2\alpha}$ stock solution (30 μg/μL dissolved in DMSO).

To test if olfactory sensory is necessary for perceiving reproductive female cues, 3M Vetbond Tissue Adhesive was used to block the nostrils in adult males. Briefly, adult males were anaesthetized using MS222, and one drop of Tissue Adhesive was applied to each side of nostril opening (Figure 1A). Fish were then released to a recovery tank with aeration tank water for 30 minutes. After recovery, fish were returned to their housing tanks and the preference trials were conducted within a week.

Behavioral tracking and assessing preference

IdTracker.es v1.0[97] was used to track focal males' coordinates on a frame-by-frame basis. We used the following parameters to track individual fish: number of individuals = 2, intensity threshold = 0.75, Minimum size = 600, Resolution reduction = 1, interval = 1-135000, number of frames for refs = 3000. Focal male preference for a particular side was scored as the amount of time spent in the "association zone": within 15 cm of the left or right permeable dividers. To assess the preference, we calculated the following:

Preference index

$$\frac{\#\ of\ frames\ observed\ in\ stimulus\ odor\ zone\ -\ \#\ of\ frames\ observed\ in\ control\ odor\ zone}{\#\ of\ frames\ observed\ in\ stimulus\ odor\ zone + \#\ of\ frames\ observed\ in\ control\ odor\ zone}$$

We compared the preference index in "pre-odor" and "odor" stages to assess whether fish exhibit any preference for stimulus odor. In addition to calculate preference indices, we also used Matlab (version 9.10.0.1613233, R2021a) to plot the temporal changes of X coordinate (ie, left vs. right tank side) in both pre-odor and odor stages.

Exposure of cichlid to odorants

Single adult males (>1-year-old) were transferred to a tank which contained 5 liter of clean aquarium water. Fish were acclimated in the tank overnight (~16 hours), to reduce the background signals of *fosab* expression in the OE. After acclimation, 100 mL of female conditioned water or 5 mL of amino acid mixture (Ala, Cys, His, Lys, Met, Phe, Trp, Val; 5×10^2 M each, Sigma; dissolved in clean aquarium water) were delivered via peristaltic pump, and the fish were exposed to the odorants for 30 min before rapid sacrifice and fixation.

Natural spawning assay for or113a *mutant lines*

We housed one sexually mature male (*or113a* mutant or wild-type siblings) and five sexually mature wildtype females in an 80-liter tank, separated by a barrier to control the onset of spawning. Halved terra cotta flowerpots served as shelters and spawning sites. Every tested male was acclimated in the spawning tanks for at least 24 hours to ensure they achieved dominant status and performed courtships to the females. We removed the barrier between females and the focal male every afternoon between 14:00–16:00, and recorded their interaction for 30 minutes using a Raspberry Pi camera. After 30 minutes, these eggs were flushed out from the female's mouth using a transfer pipet and then collected for egg retrieval assay (see method details section "fictive spawning assay"). We identified 12 spawning events in *or113a* mutant males, and 9 spawning events in their wild-type siblings. These videos were analyzed using Behavioral Observation Research Interactive Software (BORIS[100]), with experimenters blind to genotypes. For both males and females, we scored the number of pot entries, number of pecking bouts at anal fins (on males, containing egg spots), number of circling bouts, number of egg retrieval bouts, and the time spent in the pots. For males, we also scored the number of quivers towards females.

Analysis in behavior transitional probabilities

Behavior event frequencies were exported from BORIS file. Transitional probabilities were calculated by dividing the total number of each behavior by the number of instances in which the subsequent behavior occurred. Arrow weights in Figure S7I are only shown for transitions with probability $\geq$10%. We selected trials from nine *or113a*$^{\Delta/\Delta}$ males and nine wild-type males which naturally spawned with wild-type females. We used Mann-Whitney U tests to compare transition probabilities across groups, with Bonferroni-adjustment cutoff of $\alpha = 0.0021$ to correct for 24 transitions we observed.

Fictive spawning assay

In natural spawning events, females typically exhibited strong motivation to retrieve eggs after spawning, leaving limited opportunities to observe the test male's egg retrieval behavior. To further investigate this behavior, we designed an artificial spawning assay. The artificial spawning assays were performed in the male side of natural spawning assay tanks. We used $PGF_{2\alpha}$ injections to trigger mating behavior between the focal males and non-fertile females and then released freshly fertilized eggs to test male egg-retrieval. To have the eggs smoothly released into the spawning site for testing this behavior, we designed an egg provider in which a hole was cut at the bottom of a 1.7 mL microcentrifuge tube and connected to a 20 mL syringe through ~3 m of nylon tubing, enabling remote release of eggs without disturbing the animals. On the same day of spawning assays, freshly fertilized eggs were collected from spawning females (30-60 minutes after fertilization), and 50 eggs were transferred to the egg tube. The egg tube was then placed in the spawning site with the cap of the microcentrifuge tube closed. To begin the artificial spawning assay, one wild-type female was injected with PGF2α (1.5 μg/g of body mass) and placed into the spawning assay tanks to interact with the focal male. When the male and female performed circling behavior at least five times, we released eggs from the egg tube by depressing the syringe plunger. Assays were terminated if the female and male failed to perform at least 5 times of circling behavior because it indicated low quality of male-female interaction and often led to failure in egg retrieval and/or mouthbrooding behavior. After all eggs were retrieved by the female and/or male, a second batch of eggs (~30-40 eggs) were delivered to the front of the spawning site to assess additional egg retrieval behavior. Around 10-15 minutes after the second batch of egg release, we checked both male and female mouths to confirm whether they were brooding embryos. All assays were recorded using a Raspberry Pi camera. We successfully performed 11 artificial spawning assays in *or113a* mutant males, and 8 assays in their wild-type siblings. These videos were analyzed using BORIS blind to genotypes. For both males and females, we scored the number of pecking bouts at anal fins (on males, containing egg spots), number of circling bouts, number of egg retrieval bouts, and the time spent in the spawning sites. For males, we also scored the number of quivers to the females and the latency to retrieve first eggs.

Tissue collection and preparation for in situ hybridization (ISH)

Fish were quickly netted from their aquaria and sacrificed via rapid cervical transection. Brains and olfactory epithelium were exposed, fixed in 4% paraformaldehyde (PFA) overnight, rinsed in 1x PBS three times and then cryoprotected either in 30% sucrose prepared in 1x PBS (for brain) or in 30% sucrose prepared in 1x PBS plus 0.5M EDTA (for olfactory epithelium) overnight. Tissues were mounted in Epredia Neg-50 Frozen Section Medium (Richard-Allan Scientific) and stored at -80°C. Brains were sectioned at 30 μm and olfactory epithelia were sectioned at 12 μm on a cryostat (Microm HM550). Sections were collected onto four alternate sets of Superfrost plus microslides (VWR), air dried at room temperature overnight, and stored at -80°C in RNase free conditions until staining.

Chromogenic and dual-label fluorescence ISH

To localize gene expression in the olfactory epithelium, we performed chromogenic ISH with gene-specific digoxigenin (DIG)-labeled riboprobes. To identify the neuron populations and/or olfactory sensory neurons which were activated by odor cues, we performed dual-fluorescence ISH with the DIG-labeled riboprobe for the *fosab* gene and fluorescein-labeled riboprobes for specific cell type markers (e.g., *trpc2b* and *cnga2b*) or olfactory receptors (i.e., *or112*, *or113a* and *or113b*). Briefly, riboprobe templates were amplified from *A. burtoni* whole brain cDNA with gene-specific primers (see Table S2). Antisense RNA probes were transcribed using T7 RNA polymerase (HiScribe T7 High Yield RNA Synthesis Kit, NEB), with DIG-labeled nucleotides (DIG RNA-labeling mix, Roche) or fluorescein-labeled nucleotides (Fluorescein RNA-labeling mix, Roche). RNA probes were purified with RNeasy Mini Kit (Qiagen) and stored at -80°C until use.

For chromogenic ISH, cryosectioned tissue slides were brought to room temperature and outlined with a hydrophobic barrier using an Aqua-Hold Pap pen (Electron Microscopy Sciences). Slides were then treated with 4% PFA (20 min), 1xPBS (2 x 5 min), proteinase K solution (4 μg/ml, 30 min), 1xPBS (2 x 5 min), 4% PFA (15 min), 1xPBS (2 x 5 min), 0.1M triethanolamine-HCl (pH 8.0) with acetic anhydride (10 min), then 1x PBS (5 min). Slides were then incubated for 1 hour in pre-hybridization buffer at 60°C before probe solution in hybridization buffer was added to each slide, covered with hybrislips (Life Technologies), and incubated overnight at 60°C for ~18 hours. Following probe incubation the slides were washed at 60°C in pre-warmed 2x saline-sodium-citrate (SSC):50% formamide (2 x 30 min), at 37°C in pre-warmed 2x SSC (2 x 15 min), RNase (Qiagen) in 2x SSC (1:500,000, 30 min), 2x SSC (2 x 15 min), at room temperature of 1:1 mixture of 2xSSC: MABT buffer (10 min), then MABT (2 x 10 min). Non-specific binding was blocked with MABT containing 2% BSA for 1-3 hrs. Following blocking, slides were incubated with alkaline phosphatase-conjugated anti-DIG Fab fragments (Roche) diluted 1:5000 in blocking solution (MABT + 2% BSA) at 4°C overnight in a humidified chamber. Following incubation, the slides were rinsed in MABT (3 x 30 min) at room temperature, washed in alkaline phosphatase (AP) buffer (2 x 5 min), and developed in NBT/BCIP (Roche) solution at 37°C for 2-5 hrs. After development, slides were washed in PBS (2 x 5 min), fixed in 4% PFA for 10 min, washed in PBS (2 x 5 min), coverslipped with aqueous mounting media (Aqua-Poly/Mount, Polysciences), and allowed to air dry overnight.

For dual-fluorescence in-situ hybridization, the chromogenic ISH protocol was used until hybridization step, at which time both probes (DIG-labeled *fosab* probe and fluorescein-labeled probe) were applied in equal concentrations and incubated at 60°C overnight in sealed, humidified chambers. Slides were then washed in 60°C pre-warmed 2x saline-sodium-citrate (SSC):50% formamide (2 x 30 min), at 37°C in pre-warmed 2x SSC (2 x 15 min), RNAse (Qiagen) in 2x SSC (1:500000, 30 min), 2x SSC (2 x 15 min), at room temperature of 1:1 mixture of 2xSSC: TNT buffer (10 min) and TNT with 0.3% H_2O_2 (10 min), and TNT (2 x 10 min). To block non-specific binding, slides were incubated for 1 hour in 0.5% blocking reagent (Roche) dissolved in TNT buffer. All subsequent steps were performed in the dark. After incubation with anti-DIG HRP-conjugated Fab fragments (Roche) diluted 1:100 in blocking solution (TNT + 0.5% blocking reagent) at 4°C overnight in a humidified chamber, slides were rinsed in TNT buffer (3 x 30 min). *Fosab* development was done by incubating slides in TSA Cy3 solution (1:50 dilution in Amplification Diluent, AKOYA BioSci) for 1 hour at room temperature. After washing with TNT (2 x 5 min), quenching with 1.5% H_2O_2 in TNT (30 min) and TNT washes (2 x 5 min), nonspecific binding was again blocked by incubating slides for 1 hour at RT with 0.5% blocking solution dissolved in TNT buffer. Slides were then incubated with Anti-fluorescein HRP-conjugated Fab fragments (Roche; 1:100) for 2 hrs at room temperature, washed with TNT (2 x 5 min), and the staining for ion channel or olfactory receptor genes was developed by incubating slides in TSA Fluorescein solution for (1:50 dilution in Amplification Diluent, AKOYA BioSci) for 1 hour at room temperature. Reactions were stopped by incubating slides in TNT (3 x 5 min), counterstained with DAPI and coverslipped with aqueous mounting media (Aqua-Poly/Mount, Polysciences), and allowed to air dry overnight. Slides were imaged on a Nikon Eclipse Ti2 and a Leica SP5 X confocal microscope. FIJI was used to analyze *fosab* and OSN marker gene co-expression.[101]

Single nucleus RNA-seq of the cichlid olfactory epithelium

Preparation of single nucleus samples

Males were sacrificed by rapid cervical transection and both olfactory organs were dissected and frozen in pre-cooled 1.5 mL microcentrifuge tubes on dry ice. Olfactory tissues were stored at -80°C. A single nucleus suspension was prepared from one olfactory epithelium from each male (n = 8 suspensions; a single olfactory organ from 8 males). We selected the olfactory organs that best retained the intact tissue morphology after dissection. Single nucleus suspensions were prepared in tandem from each olfactory epithelium using a modified version of the "Frankenstein" protocol[102] for nuclei isolation from fresh and frozen tissue for snRNA-seq. We optimized reagent concentrations and protocol steps to obtain high quality single nuclei suspensions from cichlid olfactory epithelia. Nuclei suspensions were prepared on ice, using RNase-free materials and buffers. Freshly prepared buffers, tubes, and filters were chilled on ice throughout sample preparation. Standard P1000 pipette tips were used for all steps involving transfer of tissues and buffers. Pipetting steps were done gently (i.e., dropwise) to minimize mechanical damage to nuclei. Frozen olfactory epithelia were dounce homogenized with 10 strokes of a loose-fitting pestle (Wheaton) in 500 μL lysis buffer containing 10 mM Tris-HCl pH 7.5, 146 mM NaCl, 21 mM $MgCl_2$, 1 mM $CaCl_2$, 1 mM DTT, 0.1% BSA, 0.03% Tween-20, 5% Nuclei EZ lysis buffer (Sigma-Aldrich) and 1 U/μl Protector RNase inhibitor (Roche), followed by 5-minute incubation in lysis buffer. Samples were filtered with 20 μm mini strainers (pluriSelect) into 1.5 mL DNA LoBind tubes (Eppendorf) and centrifuged at 500 x *g* for 5 minutes at 4°C using a swinging-bucket rotor. After removing the supernatant, nuclei pellets were resuspended by pipette mixing in 100 μl wash and resuspension buffer containing 10 mM Tris-HCl pH 7.5, 10 mM NaCl, 3 mM $MgCl_2$, 1 mM DTT, 1% BSA, 1 μg/μL DAPI, and 1 U/μl Protector RNase inhibitor.

Single nuclei sample quality controls

For quality control, we aimed to sequence samples containing a high proportion of single nuclei (singlets) relative to multiplets (aggregates of 2 or more nuclei). We estimated the percentage of singlets recovered in each sample by counting $DAPI^+$ nuclei on C-Chip disposable hemocytometer slides (INCYTO). To estimate the total nuclei recovered in each sample, we counted singlets, doublets, triplets, and clumps (aggregates of ≥ 4 nuclei). We recovered an average 91,500 nuclei per sample, and the 8 suspensions contained 87% singlets on average, with minimal large clumps or tissue debris. To ensure the quality of the single nuclei samples prior to sequencing, the morphology and membrane integrity of singlets were visually assessed under 60X oil immersion using 10X Genomics guidelines. After confirming the singlets retained predominantly intact morphology, the 8 single nucleus suspensions were pooled into a final suspension such that each olfactory epithelium contributed an equal concentration of nuclei to the final pool.

10X Genomics barcoding, library preparation, and sequencing

Single nucleus 3' gene expression libraries were generated using the 10X Genomics Chromium Next GEM Single Cell 3' Reagent Kits v3.1 according to manufacturer's instructions. GEM well barcoding, library preparation, RNA and DNA quality controls, and library sequencing were conducted by the Advanced Genomics Technologies Core of the Brain & Behavior Institute at the University of Maryland, College Park. To decrease batch effects caused by technical processing,[103] samples from 4 individuals were pooled into each GEM well and sequenced on one flow cell. This approach was repeated with an independent set of four samples. Following GEM RT-Cleanup, cDNA was amplified using 12 PCR cycles. For library construction, 14 Sample Index PCR cycles were used. Libraries were sequenced at a depth of 200M paired reads (NextSeq 1000, Illumina).

Read alignment, UMI counting, and cell-calling

The 10X Genomics Cell Ranger 7.0 pipeline[104] was used to process the Chromium single nucleus data. The Cell Ranger pipeline used for the 3' single nucleus data consisted of cellranger mkfastq and cellranger count. First, cellranger mkfastq (a wrapper for bcl2fastq) generated FASTQ files from the raw Illumina binary base call (BCL) sequence files. Cellranger count used FASTQ files to perform read alignment to the transcriptome, barcode counting, and unique molecular identifier (UMI) counting. The *A. burtoni* genome NCSU_Asbu1 (GCF_018398535.1) was used as the reference for read alignment. Cell Ranger used the STAR aligner to align reads to the transcriptome. Confidently aligned exonic and intronic regions were then associated with annotated transcripts. We included intronic reads because single nuclei data may include many unspliced transcripts. Cell Ranger then grouped the transcriptomic reads that shared the same barcode, UMI, and gene annotation (Figure S9A). After UMI error correction and filtering, each barcode-UMI-gene combination was observed as a UMI count. Cell ranger then performed cell-calling with an algorithm based on EmptyDrops,[105] removing barcodes with low UMI counts and low RNA content, which likely represent empty GEMs. The Cellranger count pipeline also generated a filtered feature-barcode matrix containing gzipped TSV files that were used in R for secondary analyses.

Multiple nuclei identification

To identify singlet cells from doublets and triplets (deemed "troublets"), we used Souporcell,[98] taking advantage of multiple individuals' genetic variation for doublet detection, given the computed cluster cell assignments and cell allele counts. First, the aligned reads were remapped using minimap2.[106,107] To identify variants per cell, single nucleotide variants were called using freebayes,[108] and then this information was summarized as single cell variant information using vartrix (https://github.com/10XGenomics/vartrix; release version 1.1.16). Once each cell is defined by variant genotypes, the cells are clustered by genotype using the Souporcell custom script with the number of sample clusters (8) defined as the input parameter k. "Troublet" cells are filtered out in downstream analysis using these assignments.

Quality controls, data normalization, and scaling

Following Souporcell, we conducted data quality controls, dimensionality reduction, clustering, and differential gene expression analysis using the open source R package Seurat.[99] For quality control, we removed cells with Souporcell status "doublet" or "unassigned", cells that expressed fewer than 200 unique genes, and cells with mitochondrial genes exceeding 5% of the total gene count. Gene counts per cell were normalized by dividing gene counts by the total counts in each cell, then multiplying by the scale factor (10000). These values were then natural log-transformed. Following this we used ScaleData() to scale and center genes in the dataset.

Dimensionality reduction and cell clustering

Seurat identified 2000 highly variable genes to be used in principal component analysis (PCA) and other dimensionality reduction methods. For single cell and single nucleus data, PCA is used as a preprocessing step to select the principal components (PCs) that account for a majority of the variance in the data. These PCs can be applied to nonlinear dimensionality reduction methods, such as t-Stochastic Neighborhood Embedding (t-SNE) and Uniform Manifold Approximation and Projection (UMAP). We evaluated the total variational contributions of each PC calculated and visualized with an elbow plot in order to pick an appropriate cutoff to use for top PCs (Figure S9B). We observed an "elbow" between principal components 10-13, suggesting most of the biologically relevant variation was captured in the first 10-13 principal components. We used the top 13 PCs for downstream UMAP visualization and clustering. The Louvain community detection method was used to cluster cells. Seurat's FindClusters() function implements the Louvain community detection algorithm, for which we set the resolution parameter to 0.25. As the resolution increases, the number of

identified clusters increases.[14] This resolution produced 10 clusters, which we later confirmed to be biologically relevant putative cell type clusters by differential gene expression analysis and ISH.

Differential gene expression analysis

We used FindAllMarkers(logfc.threshold = 0.25, min.pct = 0.25) in Seurat to identify differentially expressed genes (DEGs) across clusters in the dataset. We identified the top 10 markers in each cluster by sorting DEGs by their within-cluster average $\log_2$ fold change value. We next aimed to visualize the identified putative cell types in the cichlid olfactory epithelium. We designed primers for selected top 10 markers using NCBI references sequences, and synthesized RNA probes for in situ hybridization (Table S2).

Gene set enrichment analysis

To gain further insight into the function of different cell populations in the OE, we performed gene set enrichment analysis using the gprofiler2 package. We used the gost() function to analyze the top 200 genes in each cluster. We then used gostplot() to visualize the enriched terms for each cluster (Table S1).

Identification of sensory transduction genes in OSNs

We identified clusters 0, 2, and 3 as OSNs because they were enriched for neuronal markers including *syt1a*. To further characterize the signal transduction components of individual OSN classes, we re-clustered the OSNs using the same methods described previously. We used Seurat's FindAllMarkers(logfc.threshold = 0.25, min.pct = 0.25) to identify DEGs in OSN clusters, and sorted DEGs by average $\log_2$ fold change. For ciliated and microvillous OSNs, we screened the DEGs to identify genes related to signal transduction. Most of the signal transduction genes we identified were within the top 10 DEGs for ciliated and microvillous OSNs, suggesting their importance in the sensory function of these neurons.

CRISPR gene targeting

Mutations were introduced into coding sequences of genes using CRISPR, following our previously published protocols.[62] Briefly, for each gene, two crRNA target sites were selected from top candidates in CHOPCHOP that recognize sequences 5′ of predicted essential domains and were synthesized by IDT (Table S2). tracrRNA was synthesized by IDT (1072532). crRNA:tracrRNA duplex (final conc. 5 μM) were delivered along with Cas9 protein (IDT, final conc. 5 μM) into single-cell embryos within 90 minutes of fertilization. Mosaic F_0 fish were screened for extent of mutation in finclip genomic DNA, and fish with high mutation rates were selected for breeding.

Behavior recordings of *cnga2b*$^{\Delta/\Delta}$ male reproduction

To observe male-female interactions during spawning, we established continuous video recordings of *cnga2b*$^{\Delta/\Delta}$ and control sibling males. Three broods of *cnga2b*$^{\Delta/\Delta}$ and three broods of control sibling males (n = 10-15 fish per brood) were collected, and then raised in six 8-gallon aquaria separately. All males were tagged with Visible Implant Elastomer tags (Northwest Marine Technology) for identification. Raspberry Pi cameras (Raspberry Pi 3 Model B & Camera Module v2) were mounted in front of each tank to record the behavior from 06:00 (1 hour before the lights on) to 20:00 (1 hour after the light off) daily through livestreaming software. All videos were automatically saved and uploaded to the cloud for further analysis. We checked for mouthbrooding females daily and screened the videos to find spawning events. We used BORIS to analyze the behavior performance 30 min before and after egg-laying (total 1 hour), blind to genotypes. For both males and females, we scored the number of pecking bouts at anal fins (on males, containing egg spots), number of circling bouts, number of egg retrieval bouts, and the time spent in the spawning sites. For males, we also scored the number of quivers toward females. To calculate fertilization rates, all embryos were flushed from the female's mouth between 2 to 4 days-post-fertilization by using a transfer pipet, and embryos were scored as live or dead.

Barcode sequencing for genotype mutant lines

To identify mutant individuals from F_1 offspring, we performed 2-step barcode PCR. For Step 1 PCR, we amplified ~300 bp surrounding the target sites using gene-specific primers (Table S2). We append to the 5' end of the forward PCR primer an M13 sequence (5'-TGT AAA ACG ACG GCC AGT -3'), and a "pigtail" sequence to the 5' end of the reverse PCR primer (5'- GTG TCT T-3') to ensure terminal adenylation, as needed. For Step 2, we used the amplicons from Step 1 as template, and amplified with the individual-specific barcoded M13 primers (5' - ATT ACA - N_{10} barcode - TGT AAA ACG ACG GCC AGT - 3') and the same gene-specific reverse primer as for Step 1. For both Steps, we amplified samples: 94°C, 2 min; 35 X [94°C, 15 s; 55°C, 15 s; 72°C, 30 s]; 72°C, 7 min; cool to 4°C. The amplicons from all samples were pooled then purified with QIAquick PCR Purification Kit (Qiagen). The purified products were diluted to 20 ng/μL and sent for Amplicon-EZ Next Generation Sequencing (Azenta). FASTQ files were processed using CLiCKAR v1.1.0[109] and CRISPResso2.[110]

Sarotherodon melanotheron genome sequencing and comparative proteomics

Previously sequenced raw reads of *S. melanotheron* (SRR3473461, SRR3473459) and *S. galileus* (SRR7089216) were remapped to the *O. niloticus* assembly[111] (O_niloticus_UMD_NMBU; GCF_001858045.2) using bwa mem using default alignment settings (https://bio-bwa.sourceforge.net/bwa.shtml) with Picard markDuplicates. Beta OR protein sequences were identified by BLAST search using *D. rerio* Or114-1 (NP_001122054) as query in 63 representative teleost and non-teleost vertebrate species. Sequences were

aligned and organized in a phylogenetic tree (Geneious Prime) as performed previously.[50] The subset of 243 proteins that clustered with *D. rerio* Or114-1 and *Mus musculus* OR543 (NP_001011782) were realigned to measure residue conservation. Cichlid protein sequences aligned were: *O. niloticus*, XP_003460042; *N. brichardi*, XP_006782003; *M. zebra*, XP_004565107; *A. calliptera*, XP_026048685; *P. nyereri*, XP_005737586; *A. burtoni*, XP_005929492.

QUANTIFICATION AND STATISTICAL ANALYSIS

Preference behavior assays were tracked using IdTracker.es v1.0.[97] All other behavior data, including natural spawning assay for *or113a* mutant lines and fictive spawning assay, were scored and output using BORIS. Statistical differences between experimental groups were determined using Mann-Whitney U tests with $\alpha = 0.05$.

For the "analysis in behavior transitional probabilities," behavioral events were output from BORIS and the transitional probabilities were calculated by dividing the total number of each behavior by the number of instances in which the subsequent behavior occurred. Mann-Whitney U tests were used to compare transition probabilities across groups, with Bonferroni-adjustment cutoff of α=0.0021 to correct for 24 transitions we observed.

Preference index graphs (Figures 1C–1F, 4D, and 4H) represent mean ± SD with the gray squares and lines represent preference index in individual trials. The rest of column plots represent mean ± SEM.

Simple linear regression F-test was used to test the relationships between egg fertilization rates and number of circling events (Figure 4M).

Log-rank (*Mantel-Cox*) test was used to compare latency of first egg retrieval between wild-type vs. *or113a* mutant (Figure 6J).

Sample sizes in each assay were specified in the figure legend and text.

All figures were plotted in Prism GraphPad. JMP Pro v17 was used for all statistical analysis, including non-parametric (Mann-Whitney U test) analysis and principal component analysis.

Current Biology, Volume *34*

Supplemental Information

A pheromone receptor in cichlid fish mediates attraction to females but inhibits male parental care

Cheng-Yu Li, Jessica M. Bowers, Theresa A. Alexander, Kristen A. Behrens, Peter Jackson, Cyrus J. Amini, and Scott A. Juntti

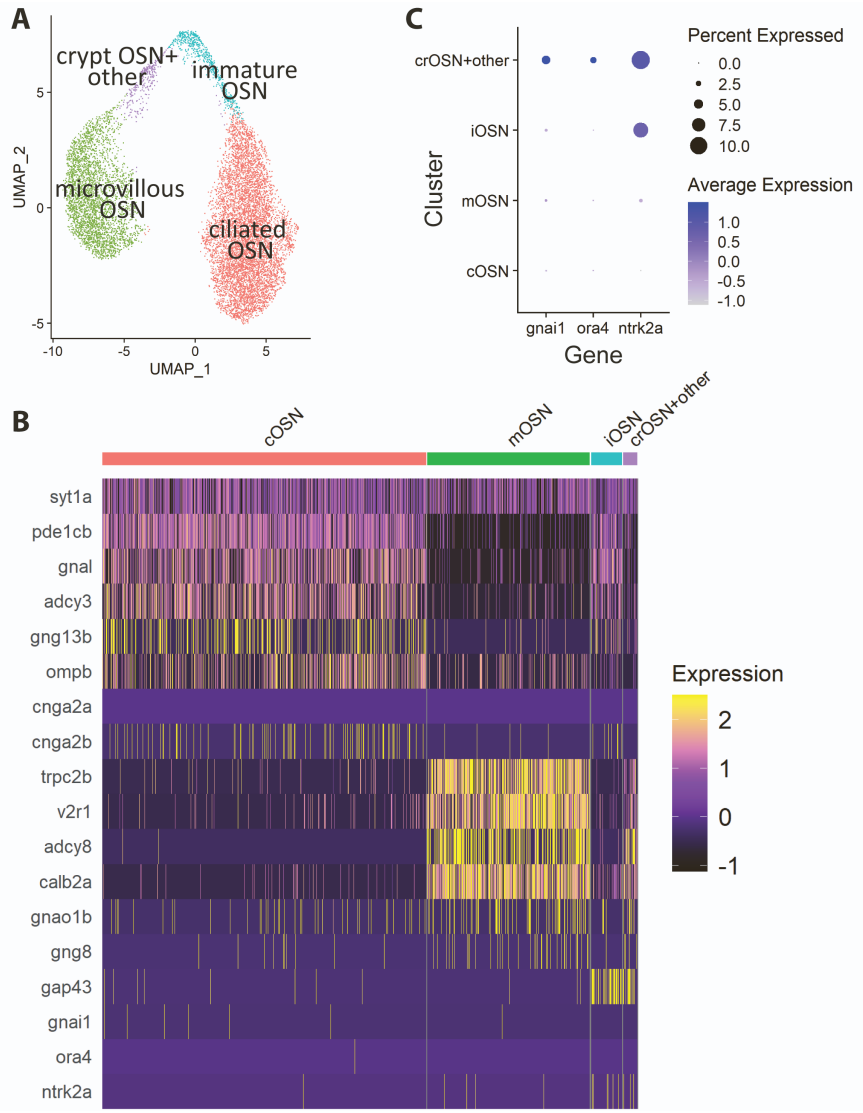


Figure S1. Olfactory epithelium cells express distinct gene profiles, 2.

(A) Re-clustered OSNs fall into 4 distinct populations.

(B) Heatmap expression of neural markers and signal transduction genes across OSN populations.

(C) Cluster 3 may represent an additional OSN population, the crypt OSNs. Known crypt OSN markers are expressed in a subset of cluster 3 neurons.

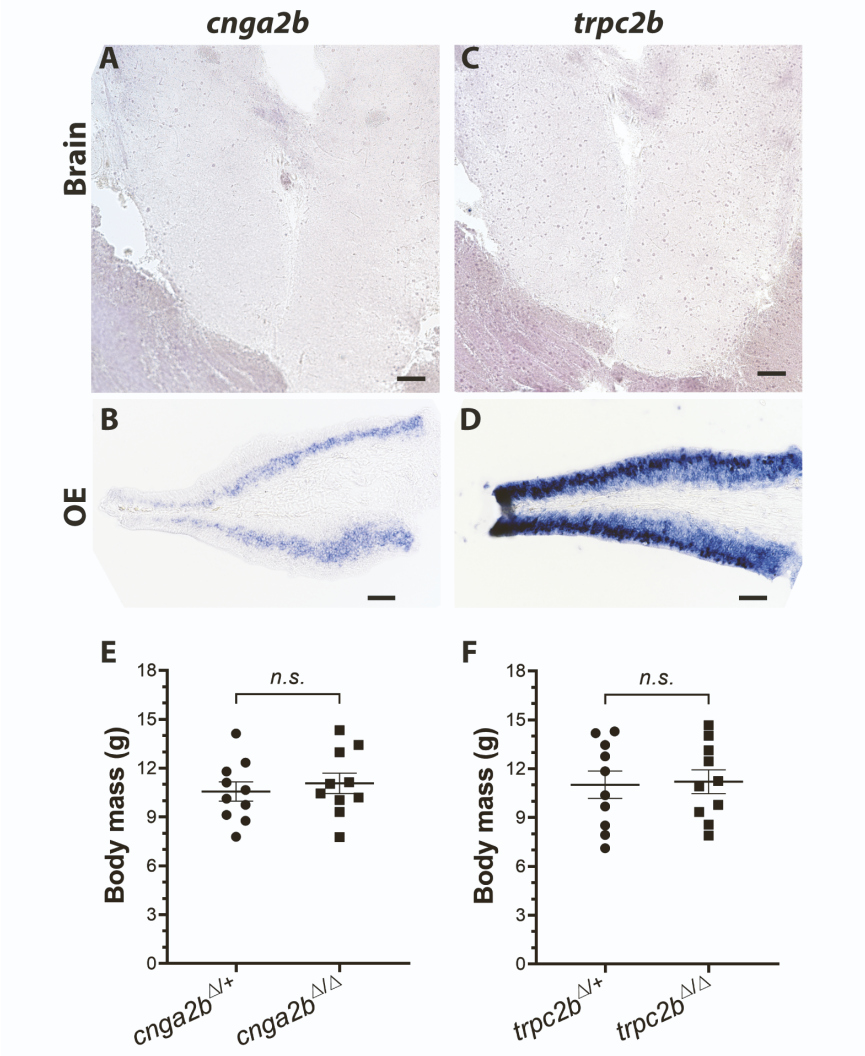


Figure S2. ISH for *cnga2b* and *trpc2b* transcripts do not reveal expression in brain, Related to Figure 3.

(A) ISH for *cnga2b* does not show labeling in the brain. Preoptic hypothalamus is shown.

(B) ISH for *cnga2b* reveals signal in the ciliated cell layer of olfactory epithelium (OE).

(C) ISH for *trpc2b* does not show labeling in the brain. Preoptic hypothalamus is shown.

(D) ISH for *trpc2b* reveals signal in microvillous cell layer of OE.

(E-F) Manipulating (E) *trpc2b* or (F) *cnga2b* genes does not influence body mass.

Mann–Whitney U test, Mean ± SEM. n = 10 fish per experiment. n.s., not significantly different across genotypes. Scale bar, 100 μm in brain, 20 μm in OE.

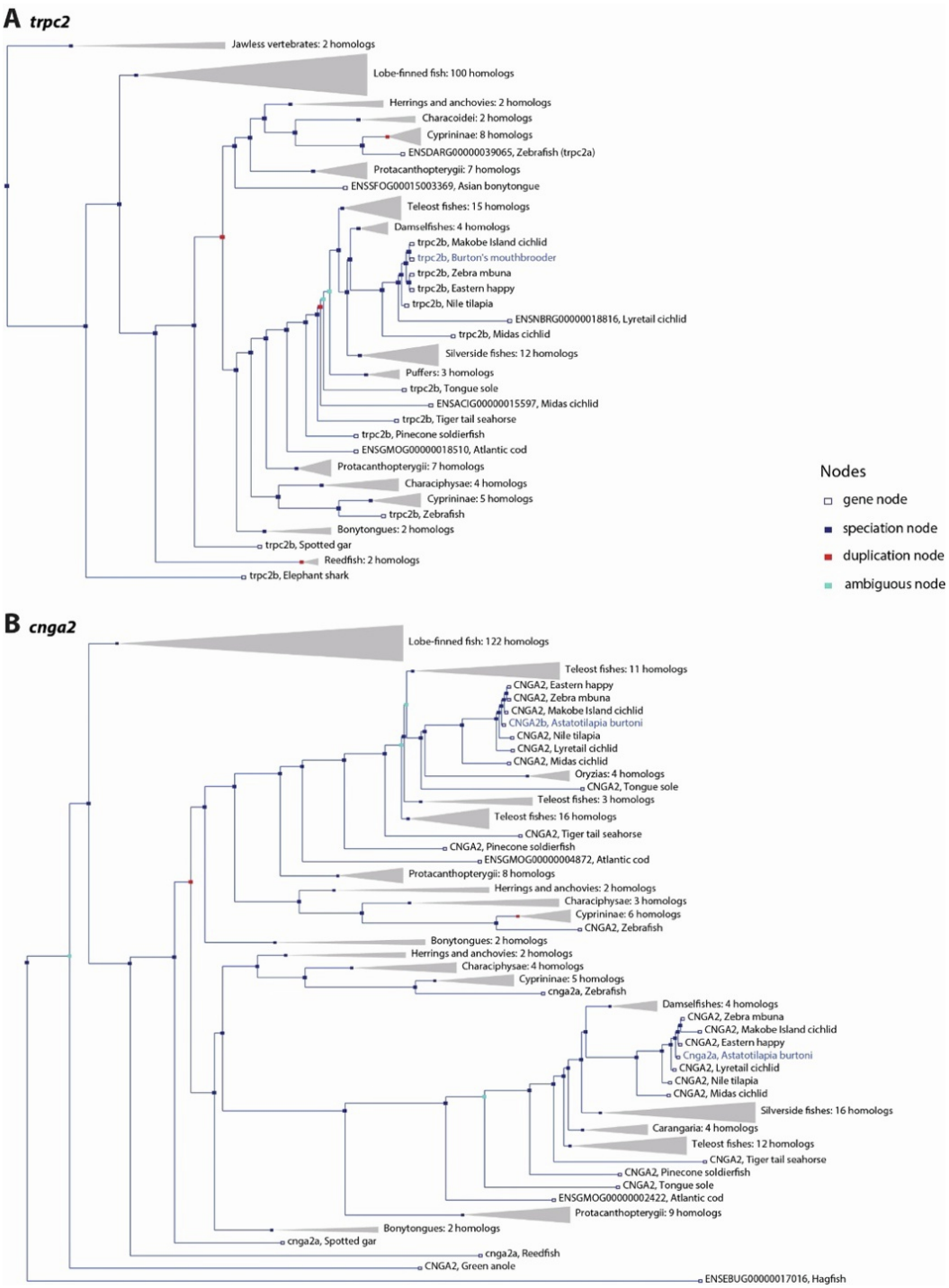


Figure S3. *cnga2* and *trpc2* genes were duplicated among teleost fishes, Related to Figure 3.

(A) Gene paralogs of *trpc2* arose early in teleost evolution, but *trpc2a* was subsequently lost in the lineage leading to cichlids. Bonytongue fish carry each paralog but gar carry only one; as these fish diverged ~240 and ~300 Mya, it suggests the duplication occurred between those time points. As cod possess only one paralog, but salmon (Protacanthopterygii) have two, it suggests that *trpc2a* was lost 150-225 Mya along the neoteleost lineage.

(B) Ancestral *cnga2* was duplicated around the teleost whole genome duplication, and two paralogs of this gene are retained in cichlids.

Trees derived from Ensembl release 110.

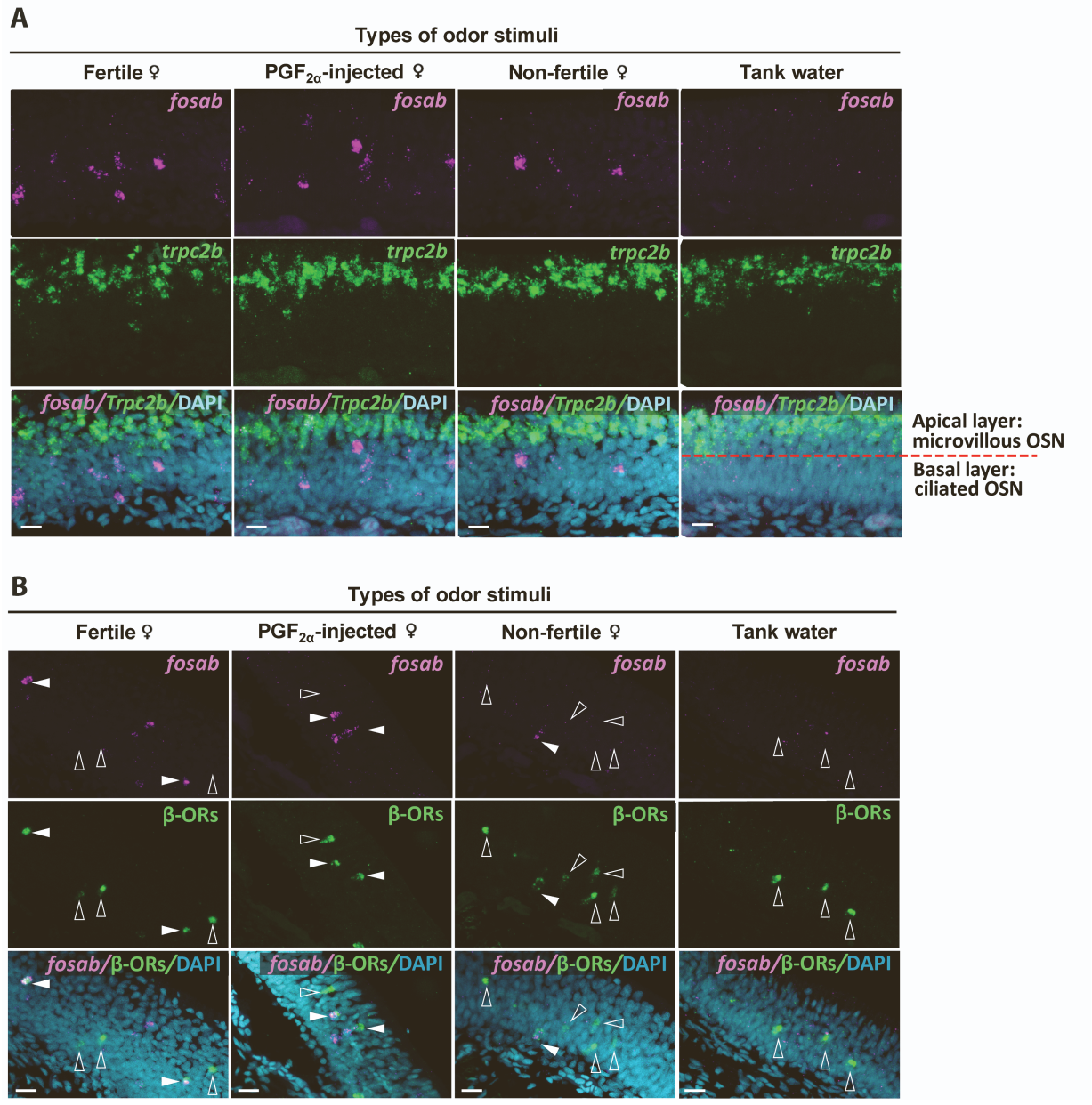


Figure S4. Screening for OSNs activated by fertile female cue, Related to Figures 4 and 5.

(A) *fosab*$^{+}$ cells are mostly located in layer of ciliated olfactory sensory neurons (OSNs) following exposure to fertile female or $PGF_{2\alpha}$-injected female. Scalebar, 10 μm.

(B) A subset of OSNs labeled by a pool of β OR transcript probes (*or112, or113a*, and *or113b*) express *fosab* mRNA following exposure to water conditioned by fertile female or $PGF_{2\alpha}$-injected female. White arrowheads indicate the neurons co-expressing a β OR gene and *fosab*. Open arrowheads indicate the neurons expressing a β OR gene but not *fosab*. Scale bar, 10 μm.

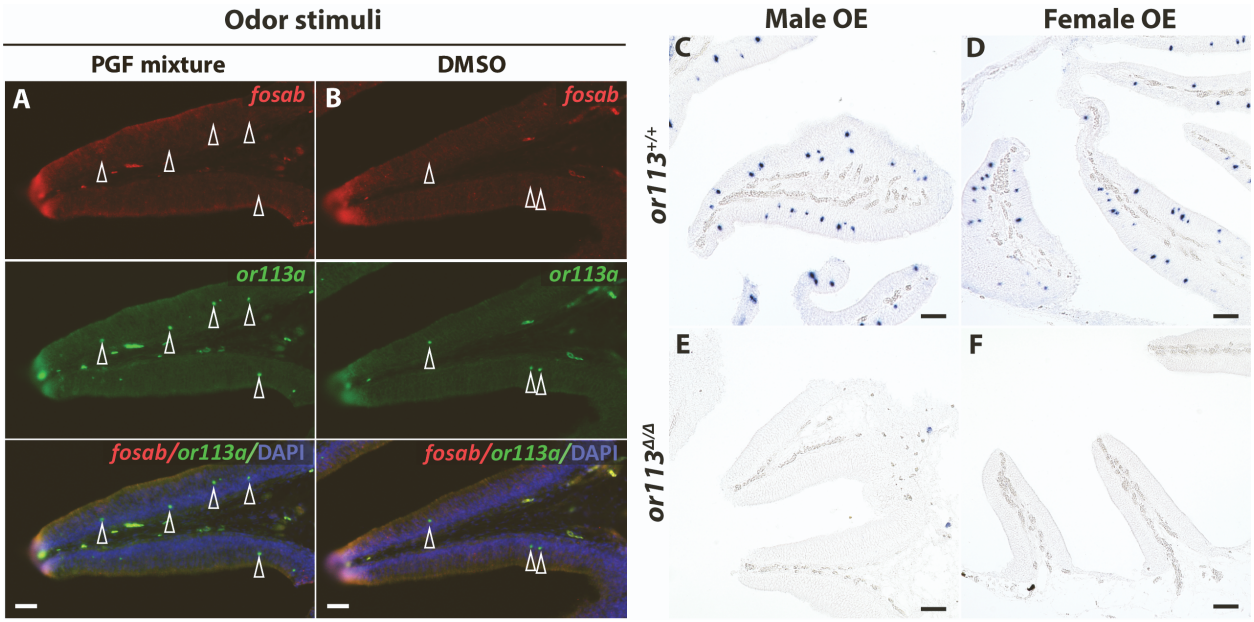


Figure S5. $PGF_{2\alpha}$ and its known metabolites do not activate *or113a*$^{+}$ cells, Related to Figure 5.

(A) A mixture of prostaglandin $F_{2\alpha}$ and known metabolites (15-keto prostaglandin $F_{2\alpha}$, 13,14-dihydro-15-keto prostaglandin $F_{2\alpha}$, 13,14-dihydro prostaglandin $F_{2\alpha}$, 19(R)-hydroxy prostaglandin $F_{2\alpha}$, 20-hydroxy prostaglandin $F_{2\alpha}$) do not activate *or113a*$^{+}$ cells. Open arrowheads denote neurons expressing *or113a* but not *fosab*.

(B) DMSO dissolved in clean aquarium water serves as a vehicle control stimulus compared to PGF mixture.

(C-F) CRISPR-induced mutations in *or113a* result in loss of gene expression. *In situ* hybridization for *or113a* mRNA. **(C)** WT males and **(D)** WT females express *or113a* mRNA in a sparse pattern across the OE. **(E)** *Or113a*$^{\Delta/\Delta}$ males and **(F)** *Or113a*$^{\Delta/\Delta}$ females do not express *or113a* mRNA in the olfactory epithelium.

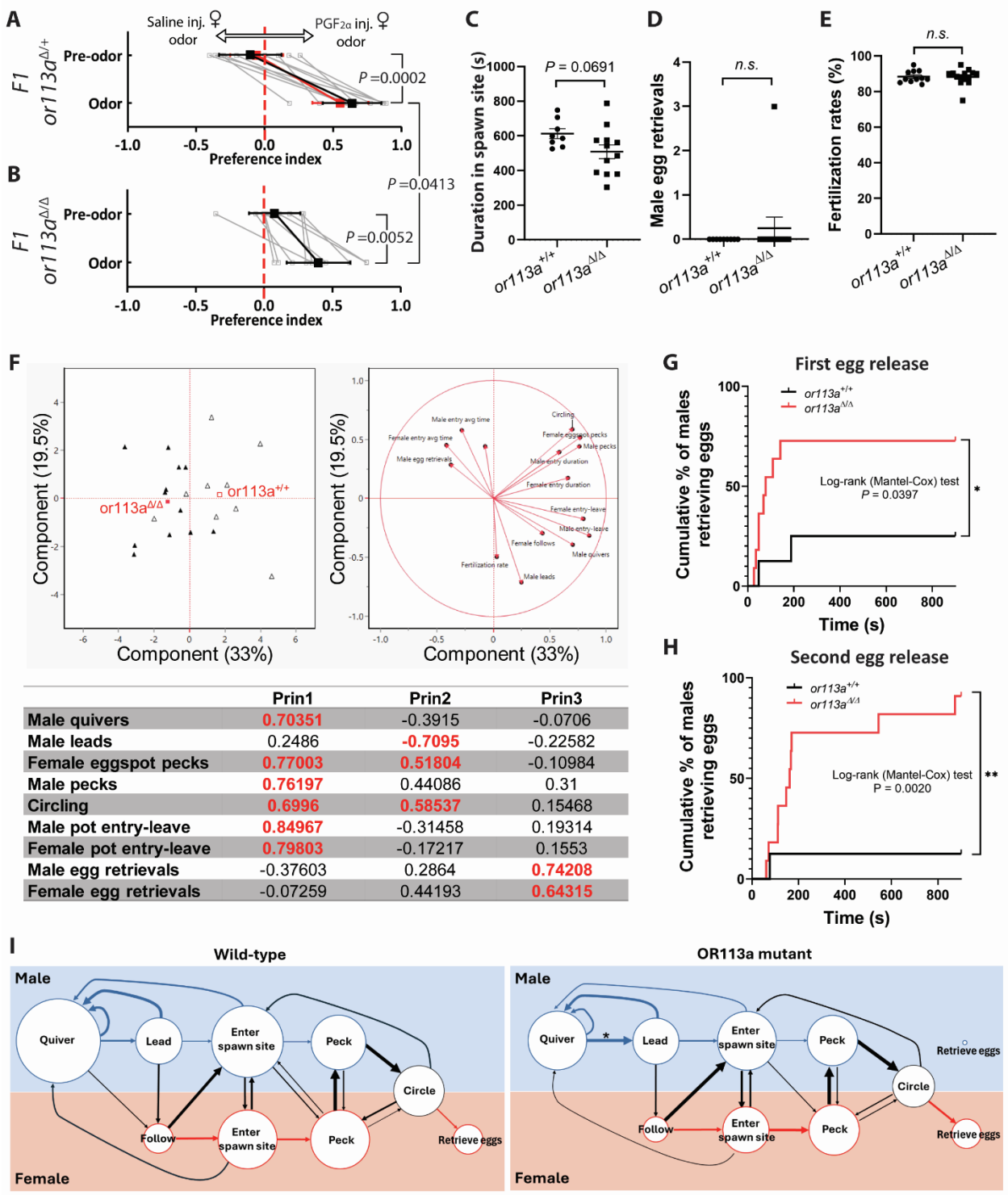
Scale bars, 50 µm.



Figure S6. Phylogeny for *or113* gene paralogs, Related to Figure 5.

A duplication of an *or113* gene occurred prior to divergence of Anabantiform and cichlid lineages, indicating that this event occurred ~100 Mya. Trees derived from Ensembl release 110. Reedfish, *Erpetoichthys calabaricus;* Spotted gar, *Lepisosteus oculatus;* Goldfish, *Carassius auratus;* Golden-line barbel, *Sinocyclocheilus graham;* Zebrafish, *Danio rerio;* Common carp, *Cyprinus carpio;* Denticle herring, *Denticeps clupeoides;* Gilthead seabream, *Sparus aurata;* Ballan wrasse, *Labrus bergylta;* European seabass, *Dicentrarchus labrax;* **Burton's mouthbrooder**, ***Astatotilapia burtoni****;* Makobe Island cichlid, *Pundamilia nyererei;* Zebra

mbuna, *Maylandia zebra;* Eastern happy, *Astatotilapia calliptera;* Lyretail cichlid, *Neolamprologus brichardi;* Nile tilapia, *Oreochromis niloticus;* Midas cichlid, *Amphilophus citrinellus;* Lumpfish, *Cyclopterus lumpus;* Barramundi perch, *Lates calcarifer*; Sheepshead minnow, *Cyprinodon variegatus.*



	Prin1	Prin2	Prin3
Male quivers	0.70351	-0.3915	-0.0706
Male leads	0.2486	-0.7095	-0.22582
Female eggspot pecks	0.77003	0.51804	-0.10984
Male pecks	0.76197	0.44086	0.31
Circling	0.6996	0.58537	0.15468
Male pot entry-leave	0.84967	-0.31458	0.19314
Female pot entry-leave	0.79803	-0.17217	0.1553
Male egg retrievals	-0.37603	0.2864	0.74208
Female egg retrievals	-0.07259	0.44193	0.64315

Figure S7. Additional behavioral results for *or113a* mutants, Related to Figures 5 and 6.

(A-B) Odor preference in F_1 offspring resulting from intercross of injected G_0 individuals. **(A)** *or113a*$^{\Delta/+}$ and **(B)** *or113a*$^{\Delta/\Delta}$ mutant males each prefer water conditioned by $PGF_{2\alpha}$-injected females over saline-injected females. However, *or113a*$^{\Delta/\Delta}$ males have reduced preference index compared to *or113a*$^{\Delta/+}$ male siblings. Gray squares and lines represent preference index in individual trials, while black squares and lines represent mean ± SD. Red squares and lines replot mean ± SD of F_2 *or113a*$^{+/+}$ from Figure 5D, indicating that

or113a heterozygosity does not affect preference. Mann–Whitney U test, n = 10 fish per experiment.

(C) In natural spawning assays, *or113a*$^{\Delta/\Delta}$ males spent less time in the spawning sites, but this difference is not statistically significant.

(D) In natural spawning assays, one *or113a*$^{\Delta/\Delta}$ male retrieved eggs, while none of the *or113a*$^{+/+}$ performed this behavior.

(E) *or113a*$^{\Delta/\Delta}$ males fertilize eggs at normal rates. n = 9-12 males per genotype.

(C-E) Mean ± SEM; Mann-Whitney U-test. n.s., not significant.

(F) Principal component analysis of all behavior scored from natural spawning assays. Behavior that dominantly loaded in each principal component are highlighted in bold red font.

(G) Male *or113a*$^{\Delta/\Delta}$ cichlids retrieve eggs more rapidly during circling behavior than *or113a*$^{+/+}$ siblings. First egg release occurs during 5th circling bout between male and female.

(H) Following retrieval of all eggs during circling behavior, *or113a*$^{\Delta/\Delta}$ males retrieve a second released set of eggs more rapidly than *or113a*$^{+/+}$ siblings. Time zero denotes the point of second egg release. Second egg release occurs 300-600 seconds after all of the first batch of eggs were retrieved by male and/or female.

(G-H) Mantel-Cox test for change in latency of retrieval.

(I) Ethograms reveal that *or113a*$^{\Delta/\Delta}$ males and their WT siblings exhibit quantitatively similar transitions between reproductive behaviors, except the transition from quiver to lead that is more frequent among *or113a*$^{\Delta/\Delta}$ males than WT siblings. Diameters of circles are proportional to count of each behavior; weights of arrows are proportional to fraction followed by the next behavior. All Mann-Whitney U-test *P*-values > 0.05 following Bonferroni adjustment, except quiver-lead $P = 0.019$. n = 9 trials per group.

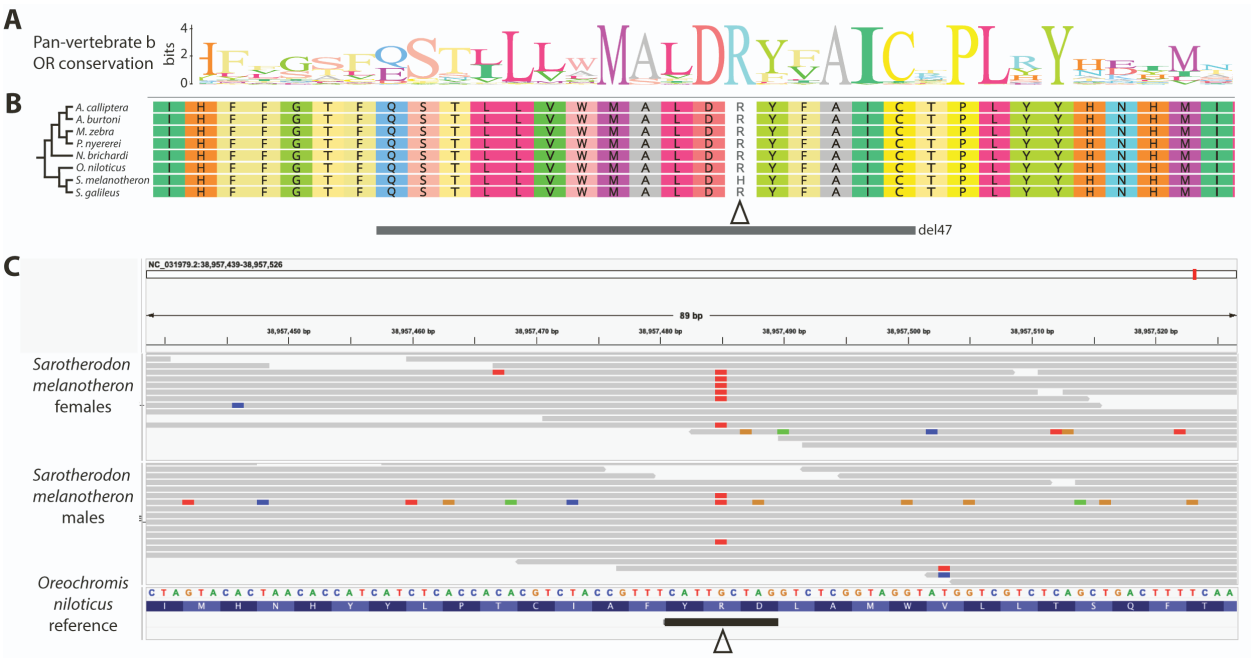


Figure S8. Putative loss-of-function mutation in ultraconserved residue of *or113a* gene of paternal mouthbrooder *Sarotherodon melanotheron*, Related to Figure 6.

(A) Logo shows complete conservation of $R^{3.50}$ residue (Ballestros-Weinstein GPCR numbering) across 68 vertebrate species β ORs. DRY motif is highly conserved in all beta-class olfactory receptors across vertebrates. Arrowhead, *S. melanotheron* $R^{3.50}H$ mutation. Phylogeny shows relationships with arbitrary genetic distances.

(B) Unlike 7 sequenced cichlid species, *S. melanotheron* carries a R>H missense allele (boxed) that causes a loss of function in other GPCRs. Gray bar denotes CRISPR-induced 47 bp deletion mutation studied in *A. burtoni*.

(C) DNA from pools of 20 males and 20 female *S. melanotheron* were separately sequenced in sex-specific pools (Gammerdinger et al, 2016) and remapped to the Nile tilapia genome (*Oreochromis niloticus*). At *or113a* (LOC10708230), 9/24 unique reads (40%) at the DRY motif (black bar) exhibit a nonsynonymous G>T SNP resulting in an Arg>His residue change (arrowhead). Colors indicate alterations from *O. niloticus* reference sequence; red indicates change to T. Note that translation proceeds from right to left for *or113a* in the *O. niloticus* reference genome.

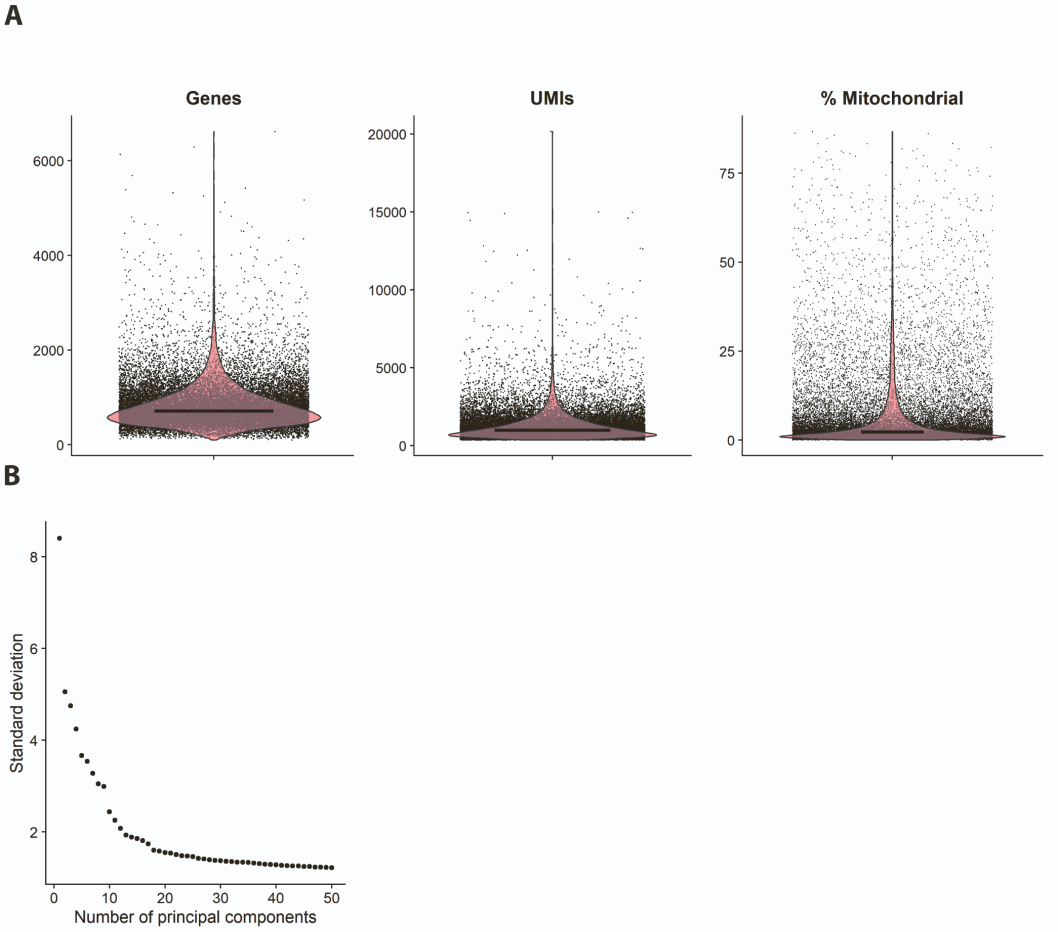


Figure S9. snRNA-seq analysis metrics, Related to Figure 1.

(A) Number of genes per cell, number of unique molecular identifiers (UMIs) per cell, and percentage of mitochondrial genes detected in the total gene count for each cell. Horizontal line denotes median value.

(B) Elbow plot correlating number of principal components (PCs) used prior to clustering nuclei. 13 PCs were used for analysis as further increase provides diminishing returns in improvement of standard deviation.

Cluster	Term ID	Source	Term name	P-value
ciliated OSN	GO:0045202	GO:CC	synapse	0.020
ciliated OSN	GO:0030054	GO:CC	cell junction	0.044
ciliated OSN	GO:0004965	GO:MF	G protein-coupled GABA receptor activity	0.049
sustentacular	GO:0016020	GO:CC	membrane	0.001
sustentacular	GO:0110165	GO:CC	cellular anatomical entity	0.001
sustentacular	GO:0005575	GO:CC	cellular_component	0.002
sustentacular	GO:0043114	GO:BP	regulation of vascular permeability	0.005
sustentacular	GO:0004725	GO:MF	protein tyrosine phosphatase activity	0.005
sustentacular	HP:0008609	HP	Morphological abnormality of the middle ear	0.018
microvillous OSN	GO:0030141	GO:CC	secretory granule	1.12E-05
microvillous OSN	GO:0099503	GO:CC	secretory vesicle	2.06E-04
microvillous OSN	GO:0045202	GO:CC	synapse	4.32E-04
microvillous OSN	GO:0048699	GO:BP	generation of neurons	7.66E-04
microvillous OSN	GO:0030133	GO:CC	transport vesicle	2.51E-03
microvillous OSN	GO:0007399	GO:BP	nervous system development	2.66E-03
microvillous OSN	GO:0030658	GO:CC	transport vesicle membrane	2.70E-03
microvillous OSN	GO:0046873	GO:MF	metal ion transmembrane transporter activity	3.50E-03
microvillous OSN	GO:0022008	GO:BP	neurogenesis	4.27E-03
microvillous OSN	GO:0016199	GO:BP	axon midline choice point recognition	5.07E-03
immature OSN	GO:0007399	GO:BP	nervous system development	7.39E-07
immature OSN	GO:0043005	GO:CC	neuron projection	1.39E-06
immature OSN	GO:0022008	GO:BP	neurogenesis	1.69E-05
immature OSN	GO:0030054	GO:CC	cell junction	3.21E-05
immature OSN	GO:0045202	GO:CC	synapse	3.34E-05
immature OSN	GO:0030424	GO:CC	axon	5.28E-05
immature OSN	GO:0031175	GO:BP	neuron projection development	9.91E-04
immature OSN	GO:0048731	GO:BP	system development	1.16E-03
immature OSN	GO:0000902	GO:BP	cell morphogenesis	1.49E-03
immature OSN	GO:0030182	GO:BP	neuron differentiation	1.52E-03
lipocalin1	GO:0048856	GO:BP	anatomical structure development	3.30E-10
lipocalin1	GO:0032502	GO:BP	developmental process	9.15E-10
lipocalin1	GO:0009653	GO:BP	anatomical structure morphogenesis	2.50E-08
lipocalin1	GO:0007275	GO:BP	multicellular organism development	2.56E-08
lipocalin1	GO:0032501	GO:BP	multicellular organismal process	6.29E-07
lipocalin1	GO:0005515	GO:MF	protein binding	1.60E-06
lipocalin1	GO:0005575	GO:CC	cellular_component	3.74E-06
lipocalin1	GO:0048731	GO:BP	system development	3.76E-06
lipocalin1	GO:0110165	GO:CC	cellular anatomical entity	4.63E-06
lipocalin1	GO:0007155	GO:BP	cell adhesion	6.48E-06
hair	HP:0012206	HP	Abnormal sperm motility	7.96E-10
hair	HP:0032543	HP	Lithoptysis	7.40E-08
hair	HP:0011539	HP	Atrial situs ambiguous	7.40E-08
hair	HP:0031456	HP	Ectopic pregnancy	7.40E-08
hair	HP:0011615	HP	Abnormal pulmonary situs morphology	7.40E-08
hair	HP:0011617	HP	Pulmonary situs ambiguus	7.40E-08
hair	HP:0025177	HP	Peribronchovascular interstitial thickening	7.40E-08
hair	GO:0008569	GO:MF	minus-end-directed microtubule motor activity	9.90E-08
hair	HP:0011535	HP	Abnormal atrial arrangement	1.00E-07
hair	GO:0030286	GO:CC	dynein complex	2.26E-07
immune1	GO:0003735	GO:MF	structural constituent of ribosome	1.21E-23
immune1	GO:0005840	GO:CC	ribosome	7.14E-23
immune1	GO:0005198	GO:MF	structural molecule activity	1.09E-17
immune1	GO:1990904	GO:CC	ribonucleoprotein complex	1.98E-16
immune1	GO:0006412	GO:BP	translation	3.38E-15
immune1	GO:0043043	GO:BP	peptide biosynthetic process	4.31E-15
immune1	GO:0006518	GO:BP	peptide metabolic process	1.02E-14
immune1	GO:0043604	GO:BP	amide biosynthetic process	4.19E-14
immune1	GO:0043603	GO:BP	amide metabolic process	5.76E-13
immune1	GO:0002376	GO:BP	immune system process	6.16E-08
immune2	GO:0044877	GO:MF	protein-containing complex binding	0.003
immune2	GO:0031683	GO:MF	G-protein beta/gamma-subunit complex binding	0.006
lipocalin2	GO:0032502	GO:BP	developmental process	0.002
lipocalin2	GO:0014037	GO:BP	Schwann cell differentiation	0.003
lipocalin2	GO:0014044	GO:BP	Schwann cell development	0.003
lipocalin2	GO:0048856	GO:BP	anatomical structure development	0.007
goblet	GO:0006887	GO:BP	exocytosis	0.002
goblet	GO:0004653	GO:MF	polypeptide N-acetylgalactosaminyltransferase activity	0.011
goblet	GO:0032940	GO:BP	secretion by cell	0.020
goblet	GO:0070161	GO:CC	anchoring junction	0.030
goblet	GO:0140352	GO:BP	export from cell	0.033
goblet	GO:0046903	GO:BP	secretion	0.035
goblet	GO:0008376	GO:MF	acetylgalactosaminyltransferase activity	0.050

Table S1. Gene ontology enrichment terms for snRNA-seq cell clusters, Related to Figure 1.
P-values displayed have been Bonferroni corrected.

Task	Gene target	NCBI Gene ID	Forward sequence	Reverse sequence	Notes
ISH	trpc2b	LOC102312590	agtcgcccagcagtacgcaatg	GAAATTAATACGACTCACTATAGGGgaaccaaagcccgtgtcctgg	T7 sequence in CAPS
ISH	cnga2b	LOC102292145	gaggcaggattgctggtggagc	GAAATTAATACGACTCACTATAGGGgctccagcagagtgacacgctg	T7 sequence in CAPS
ISH	or113a	LOC102303348	gggtttgatggccgtgtttctc	GAAATTAATACGACTCACTATAGGGcccatttggcaaatgtgacagc	T7 sequence in CAPS
ISH	apoeb	LOC102307470	TGAGATCCAGTCCCGTGCCTCC	ACTGCTCACGGATCTTGGTGGC	Product cloned into pMiniT
ISH	dnah7	LOC102293075	CACGACACCGATCGATCCTGGC	ACTGATTAAGTCAAACACCACACATG	Product cloned into pMiniT
ISH	gap43	LOC102295330	CAAACCCGAGGACAAGGCCCAC	GACTGACAGCAGCAGGCACGTC	Product cloned into pMiniT
ISH	muc2	LOC102308536	CCGCCCACAACTACCACCACAC	GGCTCTGATTCTGTGGCCCGTG	Product cloned into pMiniT
ISH	muc5ac	LOC102300516	TCAGCAGCCACCATTGTCACGG	CCTGCATGAGCACACTGACGGG	Product cloned into pMiniT
ISH	ptgdsb	LOC102304304	AGAAGCCATGAGGAGCACAC	AAGATTTGGGCTCCTCAGGC	Product cloned into pMiniT
ISH	v2r1l	LOC102296764	cggatctgtccatcgcgactgc	GAAATTAATACGACTCACTATAGGGgttgtgccacagactcctgccc	T7 sequence in CAPS
ISH	or112	LOC102302744	ccatgttggaagcaccgctaag	GAAATTAATACGACTCACTATAGGGtgagagaggaaggtgatgctgc	T7 sequence in CAPS
ISH	or113b	LOC102303044	ggggttgatctcagtcttctctg	GAAATTAATACGACTCACTATAGGGGTTCTGATGCCGTAGATGATC	T7 sequence in CAPS
ISH	ompb	LOC102290052	gcacaggagagtctggacagag	GAAATTAATACGACTCACTATAGGGcgggttcctcaactgaaagcac	T7 sequence in CAPS
CRISPR	trpc2b #1	LOC102312590	ctg cca gcc cac gaa tct ct	-	
CRISPR	trpc2b #2	LOC102312590	tcg tgt gaa gct taa cat gc	-	
CRISPR	cnga2b #1	LOC102292145	tga gtc aag gtg gaa tac cc	-	
CRISPR	cnga2b #2	LOC102292145	tat gct ata tct aag tct ct	-	
CRISPR	or113a #1	LOC102303348	tcg tgt gaa gct taa cat gc	-	
CRISPR	or113a #2	LOC102303348	gta gta aag ggg tgt gca ga	-	
Genotyping	trpc2b	LOC102312590	TGTAAAACGACGGCCAGTgcagcacgtgacaattggcacc	aagtgacctcatcatatcatcaatcatc	M13 in CAPS
Genotyping	or113a	LOC102303348	TGTAAAACGACGGCCAGTgtattctttgttccccacatgc	GTGTCTTagaacatttctgacaacaagtggta	M13 (f), pigtail (r) in CAPS
Genotyping	cnga2b	LOC102292145	TGTAAAACGACGGCCAGTggaggcatctctccaatggtggt	tcgcatctgcaacttggttctt	M13 in CAPS
Genotyping	M13-barcode		ATTACANNNNNNNNNNTGTAAAACGACGGCCAGT	-	Spacer + N10 Barcode + M13
Genotyping	M13-FAM	N/A	/56-FAM/TG TAA AAC GAC GGC CAG T	-	Universal oligo for Fluorescein addition to PCR amplicons for size analysis

Table S2. Oligonucleotides used in this study; Related to STAR methods